2008-08-06

Pre-Eruptive Conditions of the Oligocene Wah Wah Springs Tuff, Southeastern Great Basin Ignimbrite Province

Kurtus Steven Woolf
Brigham Young University - Provo

PRE-ERUPTIVE CONDITIONS OF THE OLIGOCENE WAH WAH SPRINGS TUFF, SOUTHEASTERN GREAT BASIN IGNIMBRITE PROVINCE

by

Kurtus S. Woolf

A thesis submitted to the faculty of

Brigham Young University

in partial fulfillment of the requirements for the degree of

Master of Science

Department of Geological Sciences

Brigham Young University

December 2008

BRIGHAM YOUNG UNIVERSITY

GRADUATE COMMITTEE APPROVAL

of a thesis submitted by

Kurtus S. Woolf

This thesis has been read by each member of the following graduate committee and by majority vote has been found to be satisfactory.

Date	Eric H. Christiansen, Chair
Date	Michael J. Dorais
Date	Jeffrey D. Keith

BRIGHAM YOUNG UNIVERSITY

As chair of the candidate's graduate committee, I have read the thesis of Kurtus S. Woolf in its final form and have found that (1) its format, citations, and bibliographical style are consistent and acceptable and fulfill university and department style requirements; (2) its illustrative materials including figures, tables, and charts are in place; and (3) the final manuscript is satisfactory to the graduate committee and is ready for submission to the university library.

Date	Eric H. Christiansen Chair, Graduate Committee

Accepted for the Department

Date	Michael J. Dorais Graduate Coordinator

Accepted for the College

Date	Thomas W. Sederberg Associate Dean, College of Physical and Mathematical Sciences

ABSTRACT

PRE-ERUPTIVE CONDITIONS OF THE OLIGOCENE
WAH WAH SPRINGS TUFF, SOUTHEASTERN
GREAT BASIN IGNIMBRITE PROVINCE

Kurtus S. Woolf
Department of Geological Sciences
Master of Science

The Wah Wah Springs Tuff (30.0 Ma) is one of several very large volume ash-flow tuffs (>3200 km³ of erupted magma) that were emplaced near the peak of the flare-up of activity in the Great Basin ignimbrite province of western North America. It can be characterized as a "monotonous intermediate" ignimbrite because of its intermediate concentrations of silica (~63 to ~70 wt. %), apparent uniform chemical and mineralogical characteristics, and crystal-rich nature (32 ± 10 % phenocrysts on a dense rock basis). The major phase assemblage found throughout deposit is similar to other monotonous intermediates with a few exceptions (pl > hnbl > bio, qtz >> cpx, opx > Fe-Ti oxides > ap > zcn). Based on experiments on the monotonous intermediate Fish Canyon Tuff (Johnson & Rutherford, 1989a) and this phase assemblage, the Wah Wah Springs magma

equilibrated between 775°C – 800°C. One hornblende-plagioclase thermometer with or without quartz (Holland & Blundy, 1994) and one Fe-Ti oxides thermometer (Anderson *et al.*, 1993) most consistently yield temperatures within this range. The Fe-Ti oxides oxy barometer (Anderson *et al.*, 1993) yield fO_2 estimates 2 – 3 log units above the quartz-fayalite-magnetite buffer. The Al-in-hornblende geobarometer (Johnson & Rutherford 1989b) indicates pressures between 2.0 and 2.5 kb.

Detailed compositional profiles across hornblende and plagioclase grains help constrain how intensive parameters changed during the evolution of the magma shortly before eruption. Plagioclase in the Wah Wah Springs displays oscillatory zonation (oscillations of ~An_5) with overall normal zonation. Hornblende is also zoned in Al_2O_3 and TiO_2 which typically decrease as much as 2.5 wt. % and 1 wt. % respectively from core to rim. These zoning patterns are consistent with a decrease of temperature from core to rim that accompanied progressive crystallization of a large body of magma that closely approached equilibrium.

These conditions in the parent magma for the Wah Wah Springs differ from interpretations of mineral compositions in the Fish Canyon Tuff which led Bachman *et al.*, (2002) to propose that the near solidus magma body was “rejuvenated” or reheated immediately prior to eruption. This model can not be applied to the Wah Wah Springs. Rather, the Wah Wah Springs magma appears to have been cooling and crystallizing prior to eruption.

ACKNOWLEDGEMENTS

I would like to thank all those that assisted in the completion of this work. I'm indebted to Dr. Eric Christiansen for his mentorship and the countless hours spent in guiding me and reviewing and critiquing papers. The insightful comments and assistance of Dr. Michael Dorais and Dr. Jeffrey Keith while working on this project have been of great help. Additional thanks to Dr. Dorais for his assistance with the microprobe analysis.

I would like to give special thanks to Dr. Myron Best for his thoughtful comments and unsurpassed knowledge of the Wah Wah Springs Tuff which greatly improved the quality of this work.

Final thanks go to my wife Julie and children Trevor and Lily for their unwavering support, motivation, inspiration, and understanding while "daddy" spent sometimes long hours at school.

TABLE OF CONTENTS

LIST OF TABLES

LIST OF FIGURES

INTRODUCTION

Several very large volume ash-flow tuffs (>1000 km^3 of magma) were emplaced within the Basin and Range province of western North America during the middle Cenozoic in what is known as the ignimbrite flare-up. The products of many of these eruptions have been characterized as monotonous intermediate ignimbrites (Hildreth, 1981) because of their intermediate concentrations of silica and supposedly uniform chemical and mineralogical characteristics. The combination of the crystal rich, very large volumes of tuff that were emplaced, together with the apparent uniformity of these deposits is relatively rare (Maughan *et al.,* 2002), and provokes questions as to what processes contributed to the origin, evolution, and emplacement of these ash-flow tuffs.

Recently, some geologists studying monotonous intermediates have concluded that a near solidus magma body has undergone "rejuvenation" or reheating events prior to eruption (Bachmann *et al.,* 2002; Lipman, 2007). This paradigm is also being used by others working on volcanic rocks of different compositions (Malloy *et al.*, 2008; Kennedy & Stix, 2007; Wark *et al.*, 2007). Christiansen (2005) has suggested that reheating and progressive growth of a magma body results in roof collapse and eruption. Underplating of hot, mafic magma is thought to provide the heat needed to rejuvenate the more silicic overlying magma, however, the mechanism for how the heat is transferred from the mafic magma to the more silicic magma is controversial and not fully understood (Bachmann & Bergantz, 2003; Lipman, 2007). Although poorly understood, Bachman & Bergantz (2006) do offer a "gas sparging" model as a possible explanation for thermal rejuvenation in the Fish Canyon Tuff. Further, Parat *et al.* (2008) identify the Huerto Andesite as a possible source of thermal energy required to drive such a reaction.

The Wah Wah Springs Tuff in southern Utah and Nevada is a classic example of a monotonous intermediate because of its large volume (~3200 km^3) and apparent chemical uniformity. This study investigates the possibility of "rejuvenation" shortly before eruption of the Wah Wah Springs Tuff, similar to what has been proposed for the Fish Canyon Tuff. An extensive electron microprobe survey of major phases – hornblende, biotite, plagioclase, clinopyroxene, orthopyroxene, and Fe-Ti oxides – in the Wah Wah Springs Tuff constrains the pre-eruptive temperature, pressure, and oxygen fugacity of the magma. Data obtained from these analyses is used in several geothermobarometers. These geothermobarometers are compared and contrasted to evaluate their usefulness in constraining key magma parameters. Some of these thermobarometers combined with a careful analysis of textural and zoning patterns provides a tool in constraining the intensive parameters of the magma body and how those parameters were changing shortly before eruption. Finally, the Wah Wah Springs Tuff is compared and contrasted to other monotonous intermediates around the world as well as a previous study on the Wah Wah Springs itself.

GEOLOGIC SETTING

The Wah Wah Springs Tuff is one of the three monotonous intermediates in the Indian Peak volcanic field which straddles the border of southern Utah and Nevada in the Great Basin ignimbrite province (Fig. 1). The Indian Peak volcanic field was active between 32.0 – 24.4 Ma with early and late stages of relatively small volumes of andesitic to rhyolitic lava flows and rhyolitic tuffs, while middle stages are characterized by caldera collapse and eruption of voluminous, dacitic ash-flows, or monotonous intermediates (Fig. 2), (Best *et al.,* 1989). Volcanic rocks were emplaced unconformably

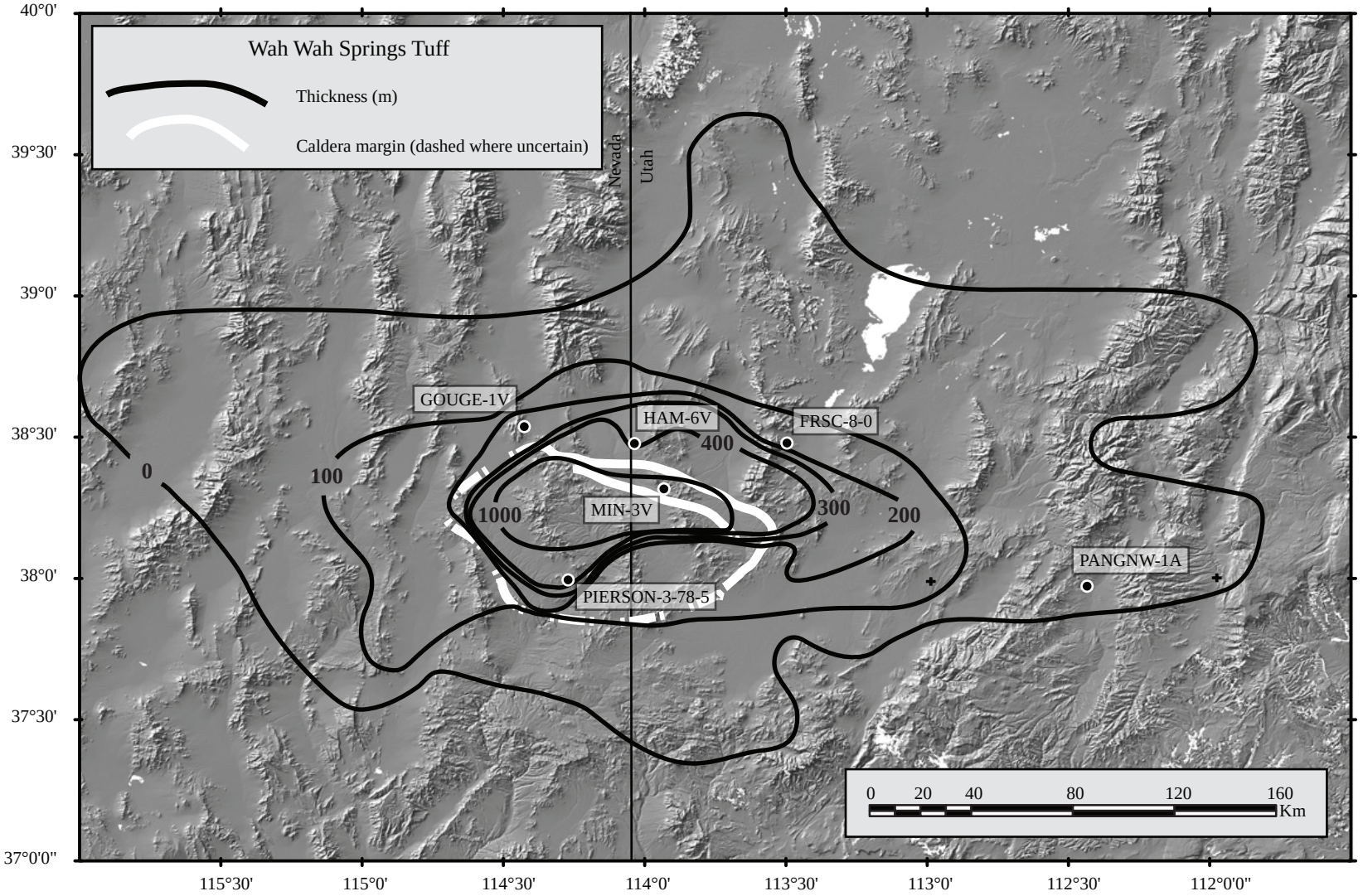

Fig. 1. Map of the Indian Peak volcanic field showing the caldera rim (white line), thickness contours in the outflow sheet (black lines), and the localities choosen for study in this investigation (black dots).

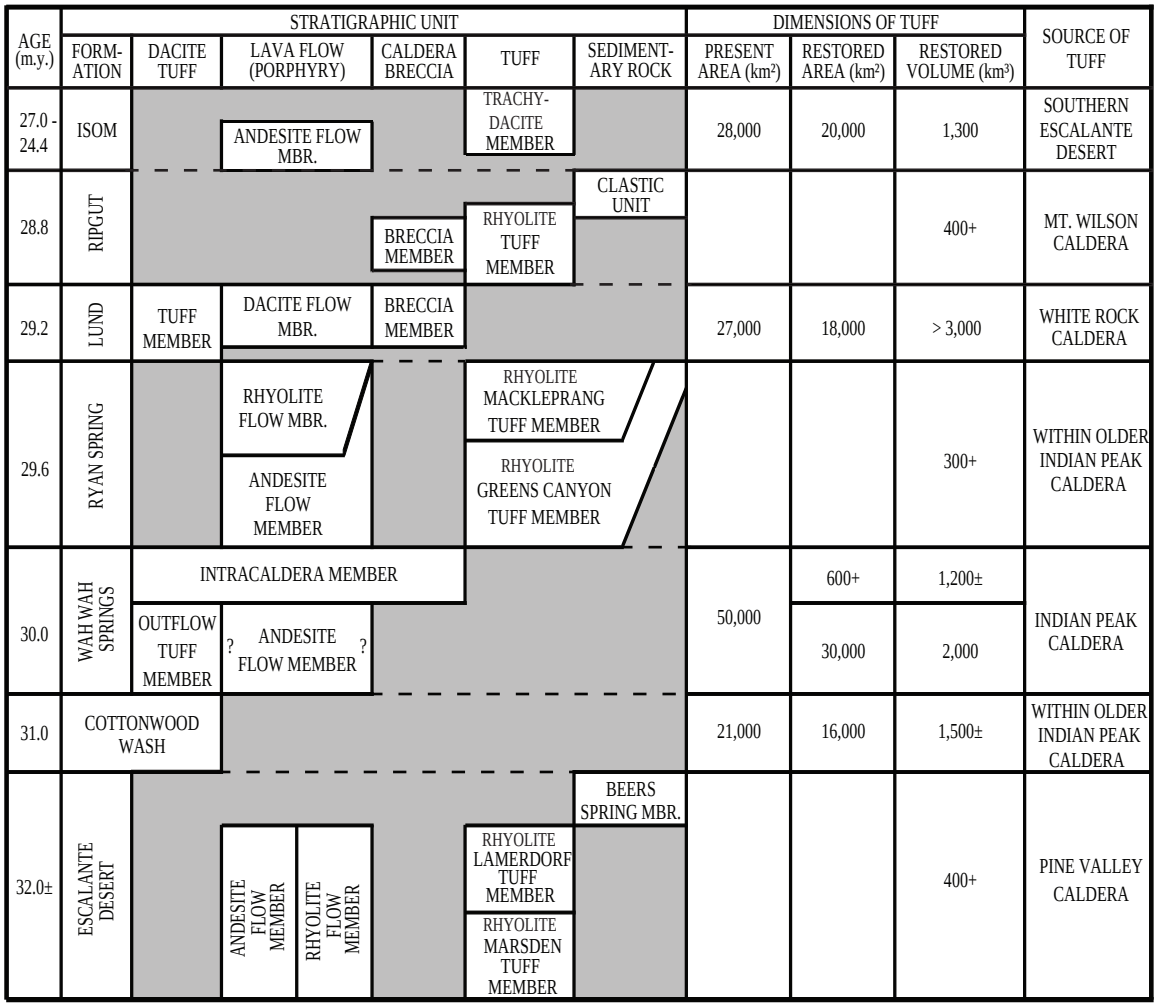

Fig. 2. A chronostratigraphic section shows the stratigraphic relations and ages of each unit from the Indian Peak volcanic field (Best et al., 1989). The vertical scale is not uniform. Restored area and volume are after correction for 50% basin and range extension.

on a thick sequence of Proterozoic through lower Mesozoic sedimentary rocks that were folded and faulted during the Cretaceous Sevier orogeny (Best *et al.,* 1989). The smaller volume tuffs of the Indian Peak volcanic field are the rhyolitic Escalante Desert (32.0± Ma, 400+ km^3), Ryan Spring (29.6± Ma, 300+ km^3), and Ripgut (28.8 Ma, 400+ km^3) Formations and the trachydacitic Isom (27.0 – 24.4 Ma, ~1,300 km^3) Formation. Small volumes of andesite and rhyolite lava are also characteristic of these formations. The very large volume formations of the Indian Peak volcanic field include the Cottonwood Wash (30.5 Ma, 1500+ km^3), Wah Wah Springs (30.0 Ma, 3200+ km^3), and Lund Formations (29.2 Ma, 3000+ km^3). These units consist primarily of dacitic ash-flow tuffs.

The Indian Peak volcanic field was one of the many active volcanic centers during the ignimbrite flare-up about 36 to 18 Ma. The ignimbrite flare-up accompanied a southward sweep of volcanism thought to be related to the subduction and removal or steepening of the Farallon plate beneath the western United States (Humphreys, 1995; Best & Christiansen, 1991). Since that time, Basin and Range extension has stretched the IPVF placing the deposits in their current locations.

Nusbaum (1990) investigated the Wah Wah Springs Tuff and made an initial petrographic analysis using textures as well as whole rock and mineral chemistry. He concluded that open-system behavior in the magma body was evidenced by high-silica rhyolite glass in conjunction with the weakly zoned phenocrysts, two distinct clinopyroxene populations, resorbed major phases, and reverse zoning in plagioclase within pumice lapilli. Temperatures were calculated using Fe-Ti oxides (Anderson & Lindsley, 1988) and pressure was estimated using the Al-in-hornblende barometer

(Johnson & Rutherford, 1989b). While the pressure estimates seem reasonable, temperature estimates appear to be anomalously high.

METHODS-ANALYTICAL TECHNIQUE

Six minimally altered samples (GOUGE-1V, HAM-6V, PIERSON-3-78-5, FRSC-8-0, PANGNW-1V, and MIN-3V) were chosen from the Wah Wah Springs Tuff and represent different parts of the large, laterally extensive deposit. The first five samples represent a basal vitrophyre from the first few meters of the base. The six samples also cover a range of bulk rock SiO_2 content spanning the range of dacite (63 – 70 wt. % SiO_2 on a volatile free basis). The first five of the six samples were chosen from different locations within the outflow tuff member. GOUGE-1V and HAM-6V are samples of a proximal outflow tuff north of the caldera. PIERSON-3-78-5 is southwest of the caldera. FRSC-8-0 is located northeast of the caldera and the PANGNW-1V is from the distal southeastern margin of the outflow sheet. MIN-3V is from the intracaldera member. Fig. 1 shows the extent of the Wah Wah Springs Tuff outflow sheet and caldera rim as well as the localities of each sample used in this investigation.

For each sample, detailed petrographic descriptions were made, paying particular attention to the textures and zoning habits of each phase. This was important in determining a change, if any, in the intensive parameters of the magma prior to eruption. Modal abundances for minor and major phases were also determined by point counting 3200 to 4300 points per sample.

Whole rock chemical analyses were obtained by X-ray fluorescence spectrometry using a Siemens SRS-303 at Brigham Young University. Major element oxides SiO_2, TiO_2, Al_2O_3, Fe_2O_3, MnO, MgO, CaO, Na_2O, K_2O, and P_2O_5 were determined by

wavelength dispersive XRF on fused glass disks. Trace elements Ba, Rb, Th, Nb, La, Ce, Sr, Nd, Sm , Zr, Cr, Ni, Sc, Zn, V, Cu, Ga, and Y were also determined by using pressed powder pellets. International reference materials were used as standards to ensure accurate results. Average compositions of standards are available from E.H. Christiansen.

Electron microprobe analyses of the hornblende (n=898), plagioclase (n=537), biotite (n=123), magnetite (n=75), ilmenite (n=38), clinopyroxene (n=63), orthopyroxene (n=52), and glass (n=68) were performed at Brigham Young University using a Cameca SX-50 instrument. Each phase was analyzed using an accelerating voltage of 15 kV. Plagioclase, Hornblende and biotite analysis were obtained with a beam current of 10 nA and beam diameter of 10 μm. Magnetite, ilmenite, and glass were analyzed under the same conditions with the exception of a beam diameter of ~2 μm. Clinopyroxene and orthopyroxene were analyzed with a 20 nA current and ~2 μm diameter. Cation abundances for hornblende were recalculated on the basis of 13 cations excluding Ca, Na, and K with Fe^{3+}/Fe^{2+} ratios calculated by charge balance (Cosca *et al.*, 1991). Plagioclase data were recalculated on the basis of 8 oxygens. Pyroxene was normalized to 4 cations per formula unit and Fe^{3+}/Fe^{2+} were calculated by charge balance (Morimoto *et al.*, 1988). Biotite formulas were calculated by normalizing to 7 octahedral plus tetrahedral cations. The methods of Stormer (1983) and Ghiorso & Sack (1991) were used to calculate Fe-Ti oxide formulas.

Complete rim-to-rim or rim-to-edge traverses over distances ranging from 169 to 1135 μm and steps of 7 to 39 μm were made across 26 euhedral to subhedral hornblende phenocrysts. A rim is identified either optically as a euhedral crystal face or from the chemical profile where there was an obvious change in major element composition from

core to rim. An edge is identified as an anhedral margin of a crystal created by fracturing or resorption; an edge can also be identified chemically if there is no or little change from core to rim in major element composition. On some larger phenocrysts more detailed rim-towards-core traverses were performed to identify subtle zoning patterns formed shortly before eruption. These traverses had distances from 27 to 167 μm and steps of 3 to 19 μm. Complete rim-to-rim or rim-to-edge traverses across 12 euhedral to subhedral plagioclase phenocrysts were made over distances ranging from 127 to 1174 μm with steps of 4 to 46 μm. Due to the difficulty of completing a traverse across some slightly altered grains, point analyses were also made on 10 other plagioclase phenocrysts. Point analyses were also made on unaltered sections of magnetite, ilmenite, biotite, clinopyroxene, and orthopyroxene phenocrysts as well as several patches of fresh glass.

WHOLE ROCK ANALYSIS

Approximately 70 samples of the Wah Wah Springs Tuff have been analyzed on a whole rock basis (Table 1). Of these, 54 are tuff samples and 16 are cognate clasts. The clasts include vesiculated pumice and dense nonvesiculated rock. The tuff samples vary in SiO_2 content from 62.5 to 70 wt. % (normalized to 100% on a volatile free basis), and thus the majority of them are dacitic in composition (Fig. 3a). A few tuff samples plot in the highest SiO_2 part of the andesite field. The majority of cognate inclusions have a smaller range of SiO_2 content from 65 to 67.5 wt. %, but one rhyolitic pumice has been found. All glass analyses are high silica rhyolites (75-78 wt. %), (Table 2). Unaltered glass was analyzed in all of the samples except for MIN-3V. The Wah Wah Springs Tuff ranges from calcic to calc-alkalic based on the modified alkali lime index (MALI) of (Fig. 3b). The tuff and cognate inclusions are dominantly metaluminous. Glass

Table 1. Whole rock major and trace element chemical analyses and modal proportions of the Wah Wah Springs Tuff.

Sample:	FRSC-8-0	GOUGE-1V	HAM-6V	MIN-3D	PANGNW-1A	PIERSON-3-78-5
wt. %						
SiO_2	64.81	69.91	67.06	64.16	64.90	63.59
TiO_2	0.58	0.43	0.52	0.65	0.61	0.68
Al_2O_3	15.11	14.03	14.70	15.59	15.84	16.06
Fe_2O_3*	5.10	3.72	4.45	5.57	5.42	5.91
MnO	0.08	0.05	0.07	0.10	0.08	0.11
MgO	3.68	1.54	1.80	2.74	2.01	2.78
CaO	4.75	3.24	4.14	4.73	5.17	5.61
Na_2O	2.36	2.63	3.27	3.16	3.02	2.51
K_2O	3.36	4.34	3.84	3.13	2.73	2.54
P_2O_5	0.17	0.12	0.13	0.17	0.22	0.21
Total	100	100	100	100	100	100
LOI	0.57	2.05	1.80	0.55	2.11	1.20
Anal Total	99.37	98.68	99.34	100.15	99.80	100.06
ppm						
Rb	116	153	139	125.	122	128
Sr	455	323	411	512	543	540
Sc	18	9	12	18	16	17
V	103	70	91	124	120	111
Cr	34	16	30	36	35	34
Ni	–	9	14	13	13	13
Cu	–	14	18	24	18	23
Zn	–	44	48	60	61	58
Ga	–	13	16	18	18	18
Y	22	16	17	17	18	23
Zr	159	157	167	171	156	172
Nb	17	14	16	14	13	11
Ba	700	730	688	728	699	727
La	36	51	50	40	35	54
Ce	94	72	80	82	81	94
Nd	31	28	39	32	34	44

Modal Proportions						
Plag	57.9	54.5	56.2	58.0	63.3	59.7
Hb	19.6	29.2	30.0	22.6	21.0	25.3
Bio	10.4	8.5	7.5	8.2	8.2	9.6
Opaques	3.8	5.1	3.7	3.6	4.3	4.3
Cpx	1.8	1.2	1.9	1.5	1.1	1.1
Opx	0.2	0.2	0.8	0	0	0.2
Quartz	6.6	0.9	0	6.2	1.9	0
San	0	0	0	0	0	0
Total Phenocrysts	42.7	24.6	26.7	45.3	39.3	44.5

Major element data has been normalized to 100% on a volatile free basis. Modal phenocrysts proportions are in respect to total phenocrysts while "total phenocrysts" are in respect to dense whole rock. Elements not analyzed are represented with "– ".

Table 2. Representative glass analyses from the Wah Wah Springs Tuff.

Sample:	FRSC-8-0	GOUGE-1V	HAM-6V	PANGNW-1A	PIERSON-3-78-5
Sample No.:	gl7	gl14	gl40	gl55	gl63
wt. %					
SiO_2	76.64	76.56	76.97	76.85	76.92
TiO_2	0.12	0.16	0.15	0.15	0.14
Al_2O_3	12.35	12.42	12.41	12.49	12.14
Fe_2O_3	0.75	0.62	0.60	0.52	0.85
MnO	0.00	0.04	0.04	0.00	0.05
MgO	0.14	0.09	0.07	0.05	0.10
CaO	0.93	0.86	0.85	0.82	0.81
Na_2O	2.26	2.31	2.45	2.59	2.61
K_2O	5.48	5.10	5.09	4.05	4.29
P_2O_5	0.00	0.00	0.00	0.02	0.02
Total	98.67	98.15	98.61	97.53	97.93

compositions are all peraluminous, perhaps because of Na loss. The tuff and cognate inclusions are magnesian while the glass samples range from magnesian to ferroan (Fig. 3c). All samples range from medium K to shoshonitic with the large majority being high K (Fig. 3d). The Wah Wah Springs Tuff plots within the volcanic arc-granite field according to the Pearce *et al.* (1984) classification (Fig. 3e) and have distinctive negative Nb anomalies. Normalized trace element patterns (McDonough & Sun, 1995) also show negative Ba, Sr, P, and Ti anomalies and decreasing enrichments of more compatible elements (Fig. 3f). The compositions of the Wah Wah Springs Tuff are similar to those of magmas formed in continental magmatic arcs and probably have a significant crustal component (Hart *et al.*, 1998). The negative Ba, P, and Sr anomalies are consistent with the removal of biotite, apatite, and plagioclase from the melt. Variations in major elements for the tuff and cognate inclusions show that the tuff isn't homogeneous (Fig. 4). MgO, Fe_2O_3, Al_2O_3, P_2O_5 and CaO increase while SiO_2 and K_2O decrease with increasing TiO_2. There is no correlation between TiO_2 and Na_2O, probably as a result of post-eruptive mobility of Na_2O. Glass compositions show no interelement correlations.

PHENOCRYST TEXTURES AND COMPOSITIONS

Similar to other monotonous intermediates (Bachmann & Dungan, 2002; Maughan *et al.,* 2002) the Wah Wah Springs Tuff appears to be nearly homogeneous throughout its very large volume, especially with regard to its phase assemblage. The samples used for this investigation are densely welded vitrophyres and contain ~2 vol. % pumice lapilli (2-5 mm) and rare lithic fragments up to 2 mm in some cases. The tuff is also phenocryst-rich containing 11% to 50% (avg. 32 ± 10%) phenocrysts on a dense rock basis. Fig. 5 displays the range of modal abundances in the Wah Wah Springs Tuff.

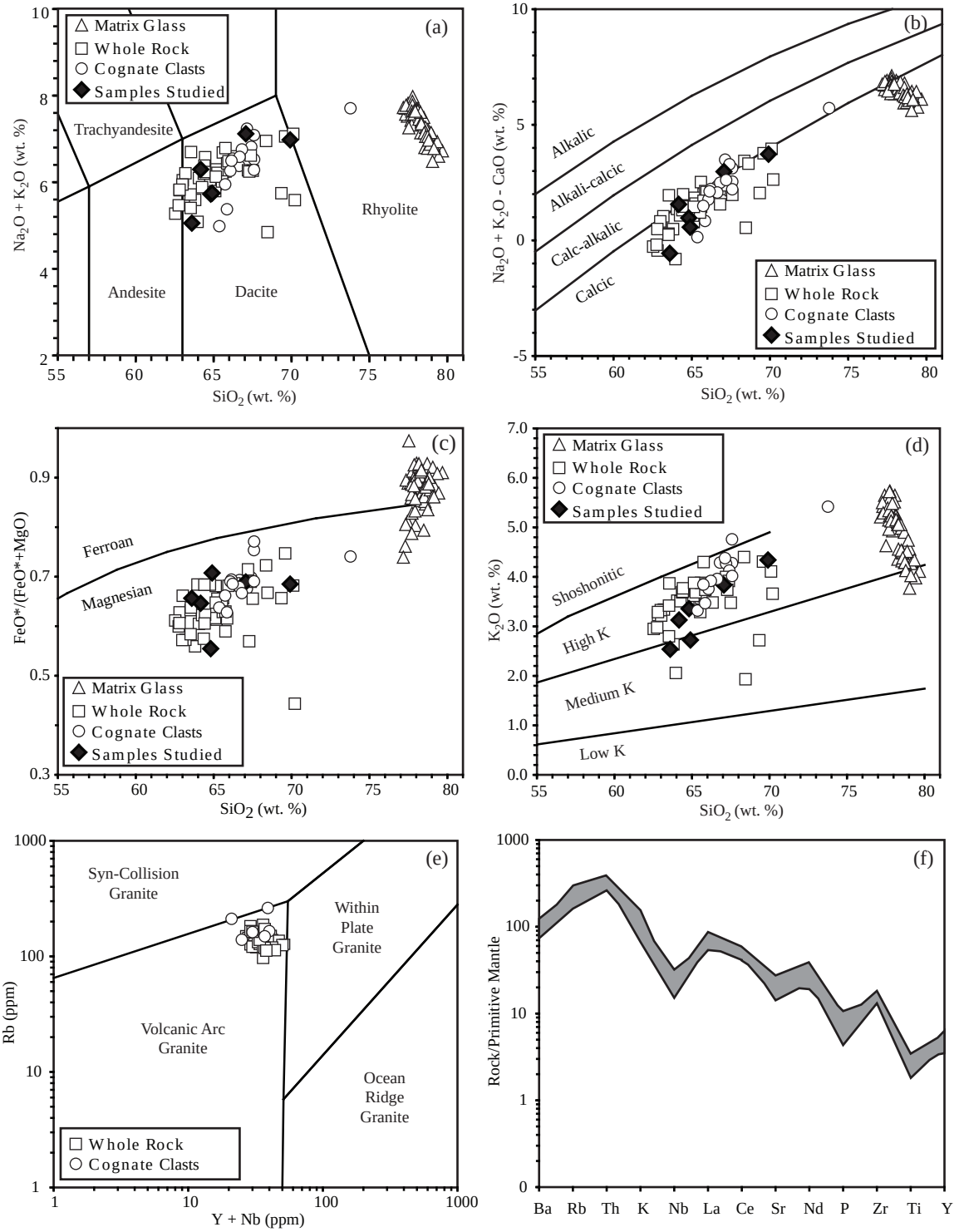

Fig. 3. Composition of the Wah Wah Springs Tuff. (a) IUGS classification of whole rock and matrix glass analyses (Le Bas, *et al.*, 1986). (b) Modified Alkali Lime Index (MALI) for whole rock and glass analyses (Frost *et al.*, 2001). (c) Ferroan/magnesian classification for whole rock and glass analyses. (d) Classification based on K_2O concentration for whole rock and glass analyses. (e) Classification of tectonic setting (Pearce *et al.*, 1984). (f) Normalized trace element pattern (McDonough & Sun, 1995) showing negative Ba, Nb, Sr, P, and Ti anomalies.

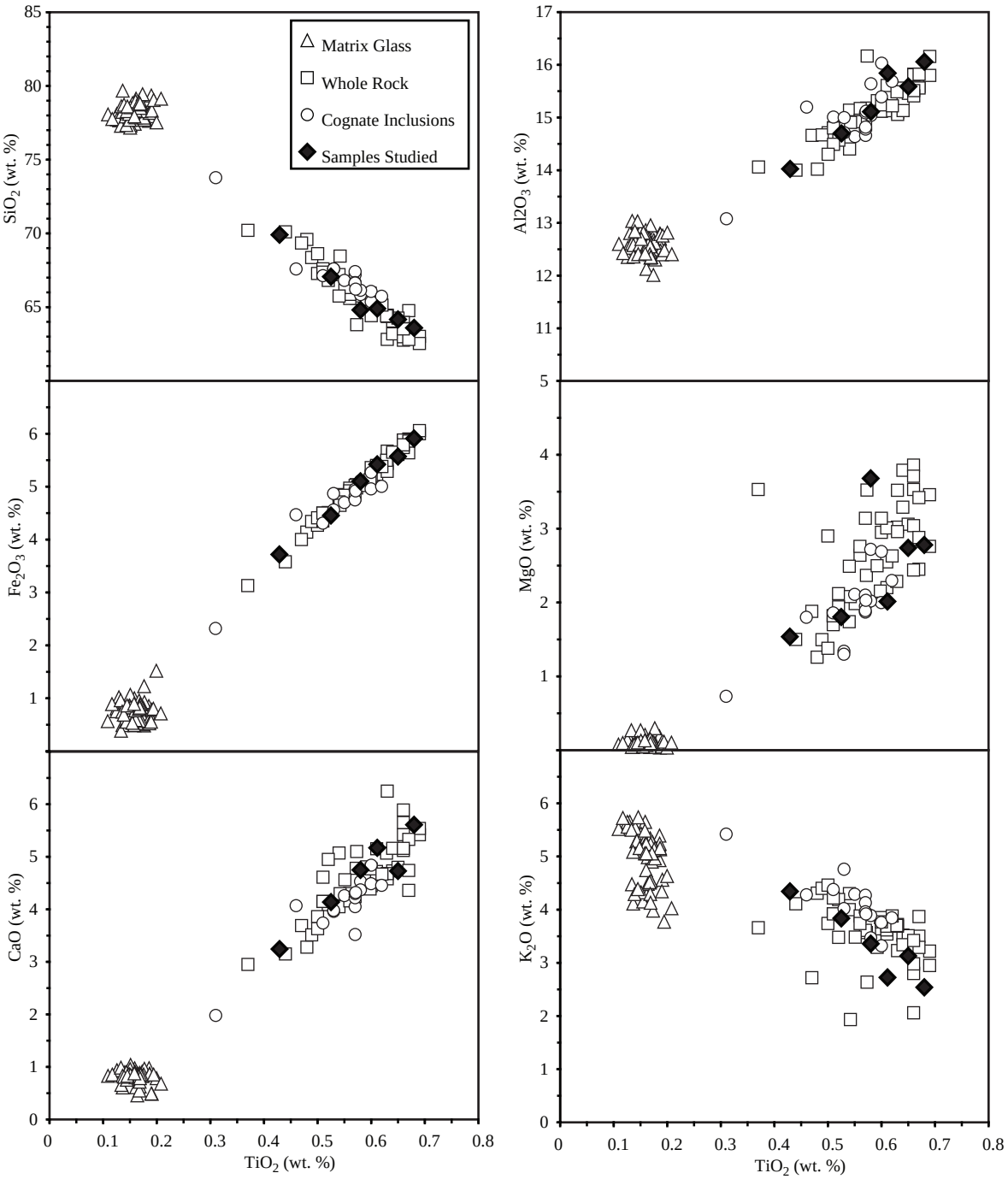

Fig. 4. Major element variation diagrams show decreases in SiO_2 and K_20 and increases in Al_2O_3, Fe_2O_3, MgO, and CaO concentrations with increasing TiO_2 for whole rock and cognate inclusions. Glass compositions show no variation. All values were normalized to 100% on a volatile-free basis.

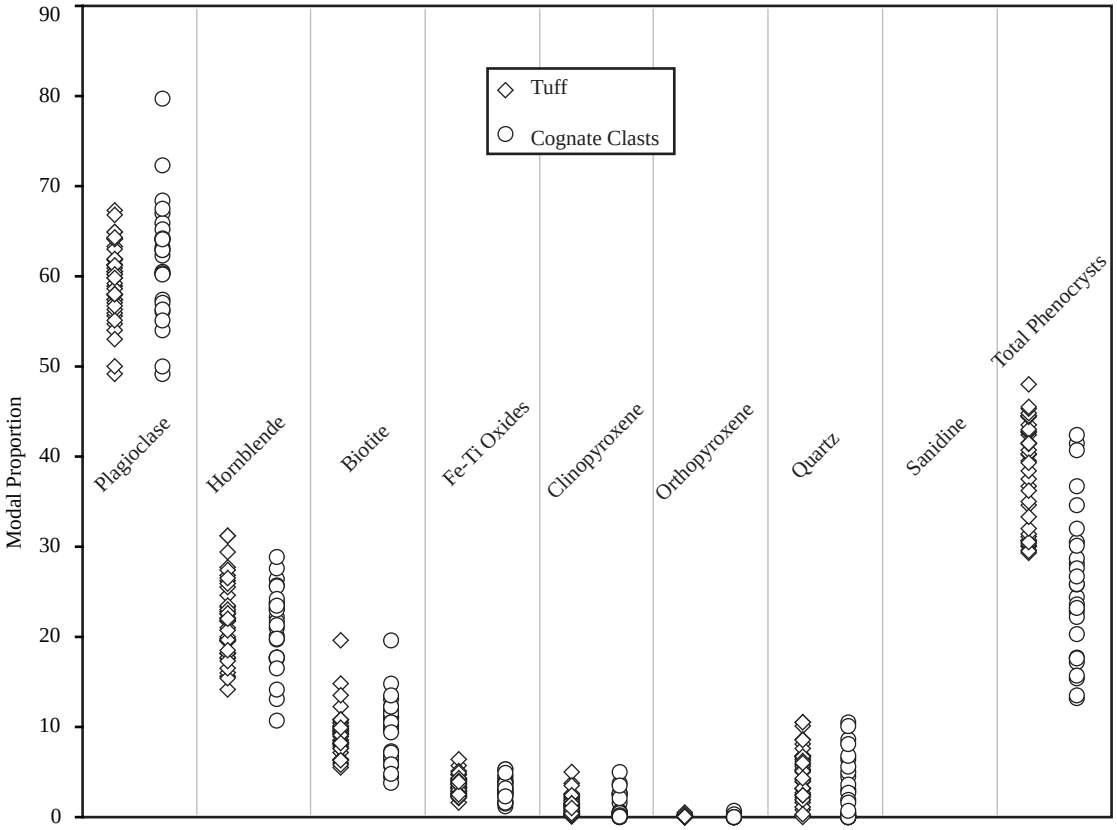

Fig. 5. Modal proportions of phenocrysts in tuff and cognate inclusions from the Wah Wah Springs Tuff. Phase percentages are with respect to total phenocrysts. Total phenocrysts are with respect to whole rock and corrected to a dense rock basis. Each data point represents an individual sample.

Phenocrysts listed in decreasing abundance are; plagioclase, hornblende, biotite, quartz, and minor clinopyroxene and orthopyroxene (Table 1). These major phases are compositionally homogenous between samples (Fig. 6). The Wah Wah Springs does not contain sanidine or titanite which are found in varying amounts in other monotonous intermediates (Bachmann *et al.*, 2002; Maughan *et al.*, 2002; Lindsay *et al.*, 2001; de Silva *et al.*, 1994; de Silva 1989; Francis *et al.*, 1989; Johnson & Rutherford, 1989a; Whitney & Stormer, 1985). Accessory minerals include Fe-Ti oxides, apatite, and zircon. Two of the samples (HAM-6V and PIERSON-3-8-5) lack quartz, and two other samples (MIN-3V and PANGNW-1V) lack orthopyroxene. (Complete sample descriptions for each sample can be found in Appendix A, and complete chemical analysis for each major phase can be found in Appendix B).

PANGNW-1V has rare xenolithic inclusions comprised of plagioclase, hornblende, orthopyroxene, and clinopyroxene. These xenoliths have different textural and chemical characteristics from the rest of the phenocrysts. Texturally, the xenoliths are holocrystalline clots of the above phases. Chemically, the hornblende, clinopyroxene, and orthopyroxene are Fe-rich compared with other analyzed grains of the same phases. The xenoliths were not considered important to the focus of this study and are not discussed further.

Plagioclase

Subhedral to euhedral plagioclase phenocrysts in the Wah Wah Springs range in size from 0.25-4 mm in length. They often display oscillatory zoning in addition to simple and polysynthetic twinning. Evidence for resorption is common as small marginal embayments. Internally, sieve texture is rare. In a few cases, highly resorbed, possibly

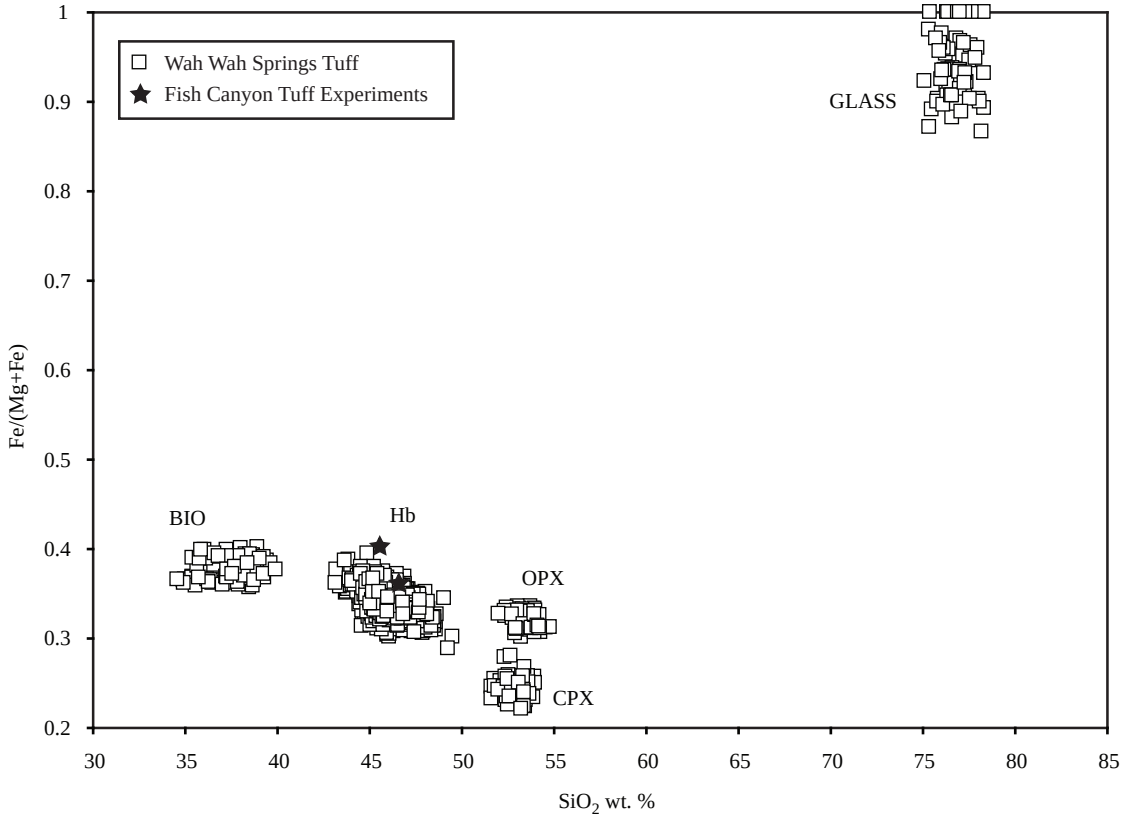

Fig. 6. Showing small variation in phenocryst and glass compositions for the Wah Wah Springs Tuff. Stars represent compositions of hornblendes in experiments from the Fish Canyon Tuff.

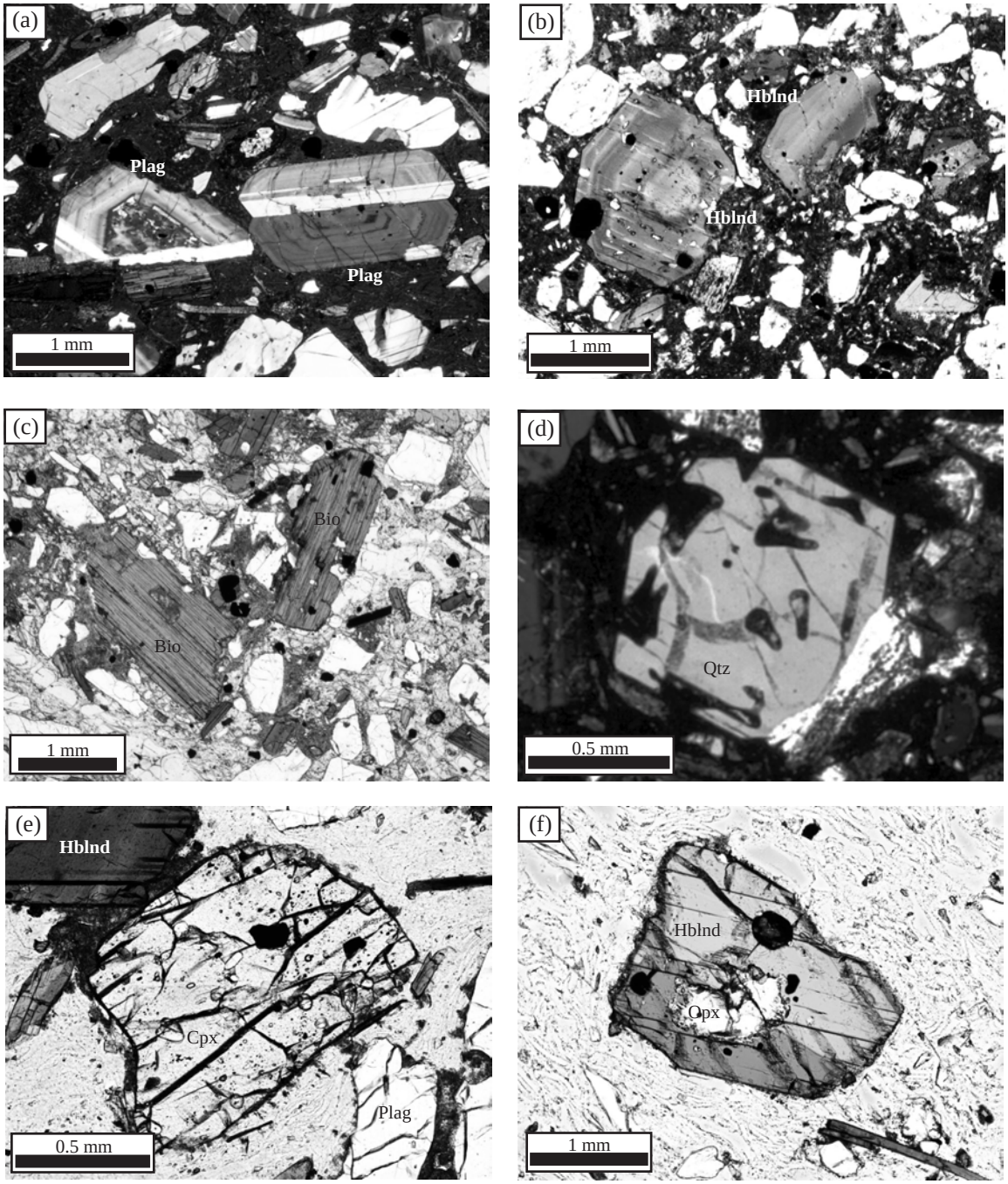

Figure 7. Representative photomicrographs from the Wah Wah Springs Tuff. (a) One oscillatory plagioclase grain overgrown on a highly resorbed "restite" core with polysynthetic twins and another euhedral composite grain showing simple and polysynthetic twins in PANGNW-1A. (b) Oscillatory zoned hornblende was only found in the intracaldera MIN-3V sample. (c) Large biotite and smaller phenocrysts of plagioclase, hornblende, Fe-Ti oxides set in a glass matrix in PIERSON-3-78-5. (d) Quartz displaying "christmas tree" texture formed by quench crystallization in MIN-3V. (e) Clinopyroxene showing slight resorption along its margins in FRSC-8-0. (f) Orthopyroxene in the core of hornblende phenocryst showing simple twinning in GOUGE-1V.

restitic, cores are overgrown by oscillatory zoned rims (Fig. 7a). Small inclusions of apatite are also found within plagioclase phenocrysts. Representative chemical analyses from plagioclase rims are shown in Table 3. Compositions of plagioclase show similar ranges between samples ranging from An_{40} to An_{70}. However, the MIN-3V sample displays a smaller range possibly due to the altered nature of the sample and the difficulty of obtaining good core analyses. Another exception to this typical range in An % is one high An core (An_{78} to An_{86}) found in PANGNW-1V (Fig. 8). Traverses across several grains show small oscillations in An content (~5%). Most grains (7 out of 12) also show a decrease of An from core to rim (Fig. 9 and Appendix C). Typical core compositions are labradorite ranging from An_{50} to An_{70}. Rim compositions are andesine ranging from An_{40} to An_{49}.

Hornblende

Hornblende phenocrysts in the Wah Wah Springs Tuff are poikilitic, mostly euhedral, and range from 0.25-2.5 mm in size. They often display simple twinning and slight optical zonation. Approximately two-thirds of analyses are magnesiohornblende while the other third are edenite in the calcic amphiboles group (Leake *et al.*, 1997). The majority of grains are normally zoned; however, in the intracaldera sample (MIN-3V) rare oscillatory zoned grains are also observed optically (Fig. 7b). Some hornblendes are overgrown on anhedral cores of clinopyroxene and orthopyroxene and other hornblende grains. Inclusions of plagioclase, apatite, zircon, and opaque minerals are abundant.

Similar to the Fish Canyon Tuff (Bachmann & Dungan, 2002), most of the variation in Al(IV) (0.8 apfu) can be explained by the temperature-sensitive edenite exchange and a derivative of the Ti-Tschermak exchange (Spear, 1981). In the Wah Wah

Table 3. Representative chemical analyses of plagioclase from the Wah Wah Springs Tuff. Each analysis is from a phenocrysts rim.

Sample:	FRSC-8-0	GOUGE-1V	HAM-6V	MIN-3V	PANGNW-1A	PIERSON-3-78-5
Sample No.:	Pl37	Pl127	Pl167	Pl370	Pl427	Pl524
wt. %						
SiO_2	57.57	55.64	55.03	57.56	55.31	55.61
Al_20_3	26.55	27.35	27.85	27.10	28.32	28.54
Fe_2O_3	0.35	0.28	0.40	0.21	0.31	0.28
CaO	8.74	9.41	10.03	8.90	9.83	10.39
Na_2O	5.93	5.61	5.58	6.38	5.80	5.68
K_2O	0.62	0.54	0.50	0.63	0.50	0.48
Total	99.77	98.83	99.38	100.77	100.07	100.98
Ab	53.10	50.24	48.74	54.49	50.17	48.40
An	43.23	46.59	48.40	41.98	46.96	48.93
Or	3.67	3.17	2.86	3.52	2.86	2.67
apfu						
Si	2.59	2.53	2.50	2.57	2.49	2.49
Al	1.41	1.47	1.49	1.42	1.50	1.50
Fe^{3+}	0.01	0.01	0.01	0.01	0.01	0.01
Ca	0.42	0.46	0.49	0.43	0.47	0.50
Na	0.52	0.49	0.49	0.55	0.51	0.49
K	0.04	0.03	0.03	0.04	0.03	0.03

Cation abundances were recalculated on the basis of 8 oxygens.

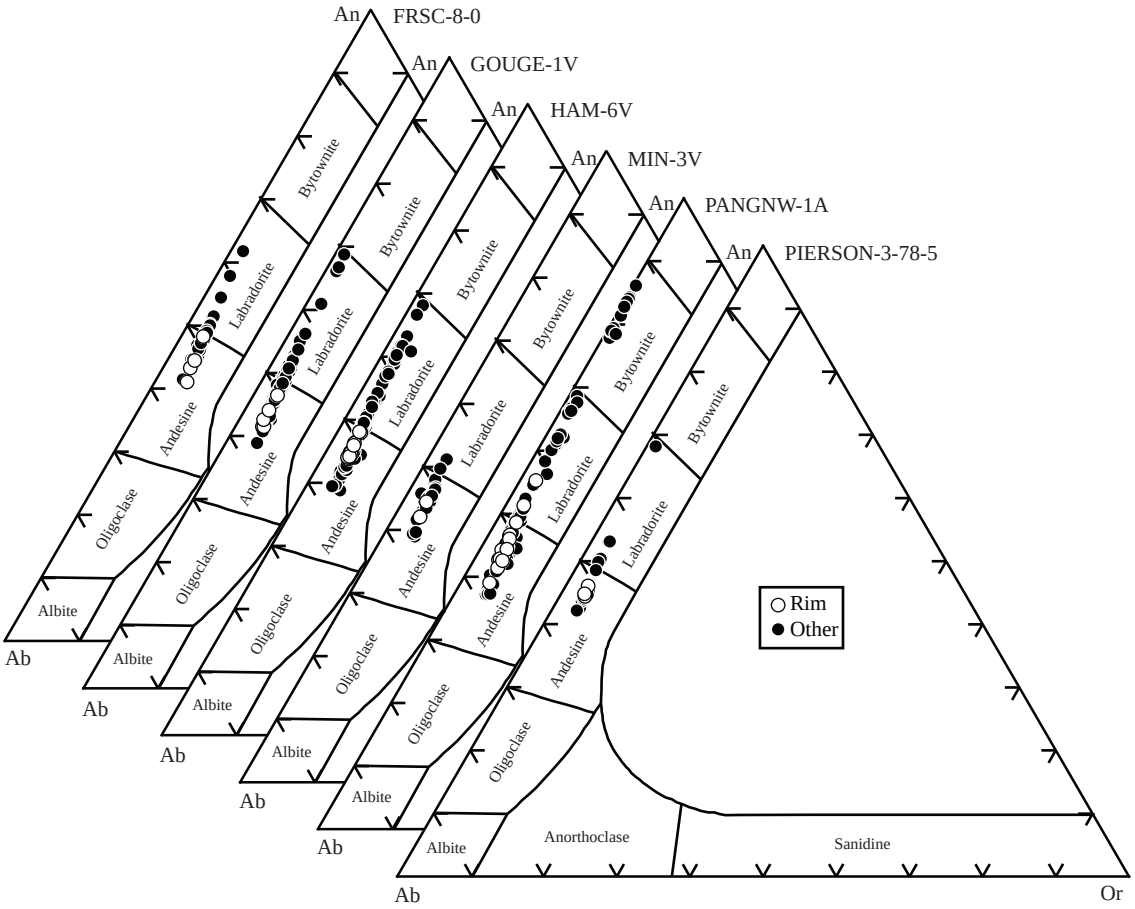

Fig. 8. Compositions of plagioclase from the Wah Wah Springs Tuff showing compositional similarities between samples. Open circles indicate rim analyses while closed represent all other analyses.

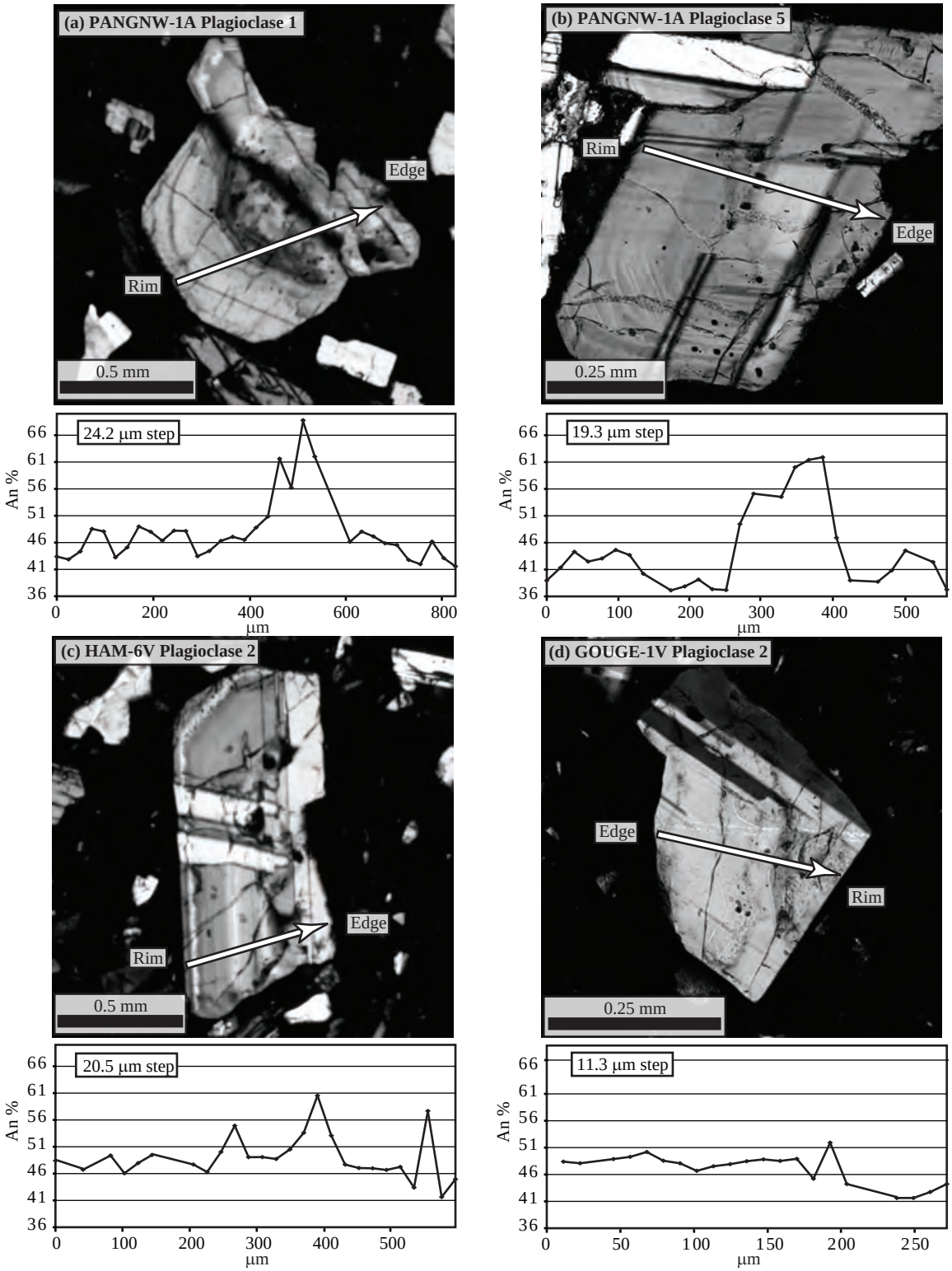

Fig 9. Plagioclase composition profiles show oscillations and an overall decrease in An content from cores to rims.

Springs the edenite exchange [Si(IV) + $^{A}\square$ = Al(IV) + ^{A}(Na+K)] accounts for about 50% of the Al(IV) variation (Fig. 10a) while the other 50% is explained by Ti-Tschermak exchange (2Si(IV) + $^{M1-M3}$Mn = 2Al(IV) + $^{M1-M3}$Ti) (Fig. 10b). Also similar to the Fish Canyon Tuff, the pressure sensitive Al-Tschermak exchange (Si(IV) + $^{M1-M3}$Mg = Al(IV) + $^{M1-M3}$Al) did not play a role in the Al variation in the Wah Wah Springs (Fig. 10c).

Hornblende in the Wah Wah Springs shows little chemical variability with Fe / (Fe+Mg) ranging from 0.29 to 0.40 between all of the samples (Table 4 and Fig. 11). Detailed traverses across 21 of 26 hornblende grains show normal zonation as evidenced by decreases in TiO_2 (~1.0 wt. %) and Al_2O_3 (~2.0 wt. %) and increases in SiO_2 (~2.0 wt. %) from cores to rims (Fig. 12a and b). This normal zonation is not seen in Fe / (Fe+Mg) as it shows little variation across hornblende phenocrysts. These changes in composition are consistent with a decrease in temperature immediately prior to eruption. The oscillatory zoned grains in MIN-3V show a similar normal zonation overprinted on the smaller oscillations (Fig. 12c). Al_2O_3, MgO, and FeO_{tot} oscillate up to 2.0 wt. % and TiO_2 up to 0.7 wt. %. An additional 5 grains show little variation in composition and elemental concentrations across the whole phenocrysts and are very similar to those in the rims of the normally zoned grains (Fig. 12d). (Traverses across all hornblende grains not found in the main body of this text can be found in Appendix D).

The occurrence of two types of hornblendes, one normally zoned and the other unzoned, could indicate two periods of crystal growth during the evolution of the magma chamber. Initially, the magma was cooling and crystallizing allowing the normally zoned grains to form. This was followed by a more steady state wherein the unzoned grains formed, during which little variation occurred in the intensive parameters of the magma

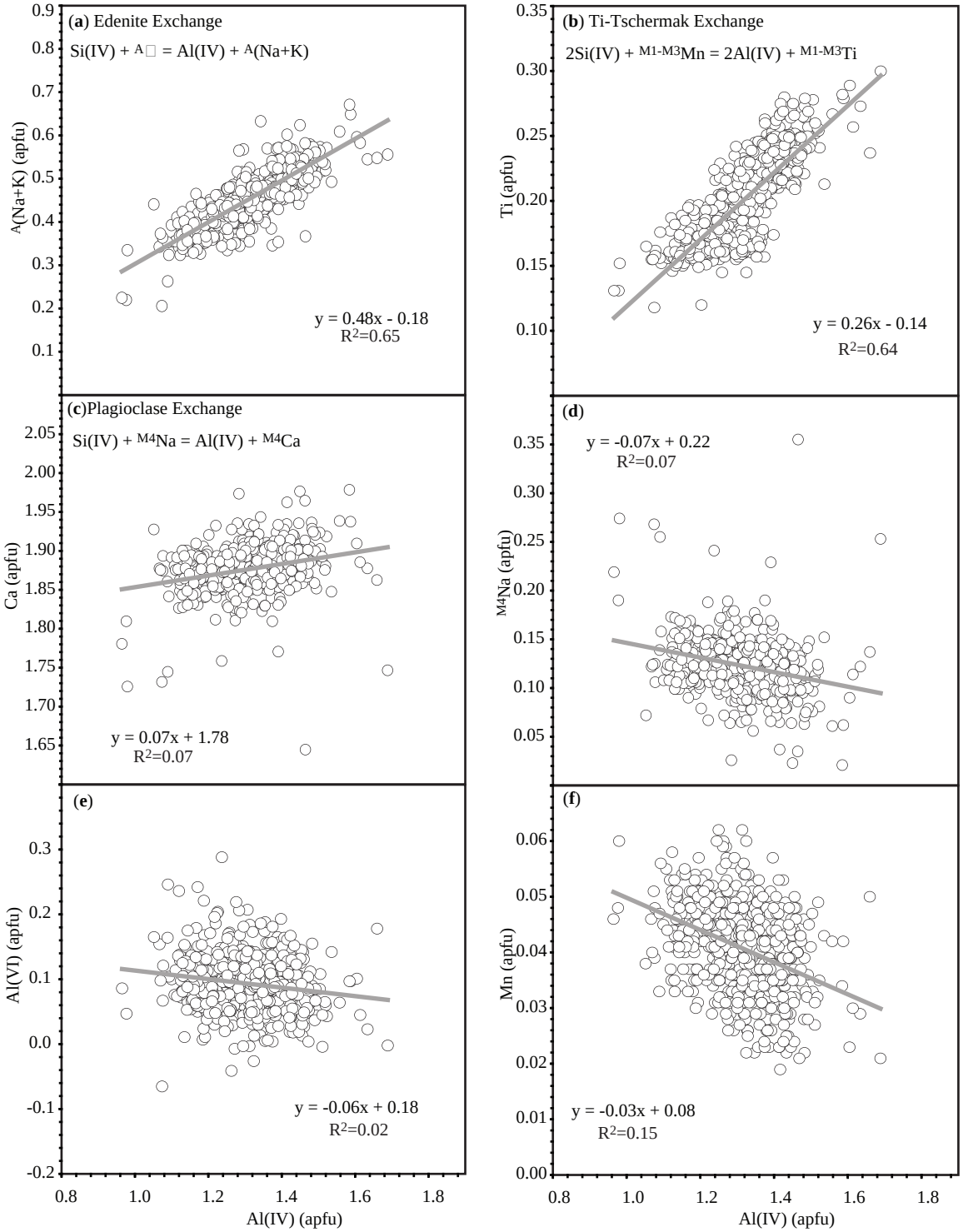

Fig. 10. Al(IV) vs (a) ^{A}(Na + K), (b) Ti, (c) Ca, (d) ^{M4}Na, (e) Al(VI), and (f) Mn diagrams show the substitution mechanisms in hornblende from the Wah Wah Springs Tuff. Slopes from regression lines plotted through the data are used to calculate the extent of each exchange.

Table 4. Representative chemical analyses of hornblende from the Wah Wah Springs Tuff. Each analysis is from phenocryst rim.

Sample:	FRSC-8-0	GOUGE-1V	HAM-6V	MIN-3V	PANGNW-1A	PIERSON-3-78-5
Sample No.:	Hb72	Hb174	Hb427	Hb504	Hb732	Hb854
wt. %						
SiO_2	47.19	47.08	47.50	46.18	46.23	47.39
TiO_2	1.51	1.45	1.43	1.53	1.57	1.70
Al_2O_3	7.58	7.74	7.17	7.75	7.61	7.42
FeO_{tot}	13.16	13.38	12.68	13.28	13.46	12.87
MnO	0.37	0.38	0.36	0.46	0.28	0.45
MgO	14.30	14.39	14.56	14.46	13.69	14.41
CaO	11.91	12.08	12.07	12.08	11.71	11.91
Na_2O	1.36	1.31	1.23	1.45	1.30	1.40
K_2O	0.80	0.80	0.73	0.86	0.91	0.83
Cl	0.09	0.10	0.06	0.12	0.08	0.09
Subsum	98.25	98.69	97.78	98.13	96.82	98.45
H_2O*	2.05	2.06	2.05	2.03	2.01	2.05
Total	100.30	100.74	99.83	100.16	98.83	100.50
Fe/(Fe+Mg)	0.34	0.34	0.33	0.34	0.36	0.33
apfu						
Si	6.82	6.78	6.89	6.71	6.81	6.84
Aliv	1.18	1.22	1.11	1.29	1.19	1.16
Alvi	0.12	0.10	0.11	0.03	0.13	0.10
Ti	0.16	0.16	0.16	0.17	0.17	0.19
Fe^{2+}	1.08	1.05	1.09	1.02	1.19	1.10
Fe^{3+}	0.51	0.56	0.45	0.59	0.47	0.45
Mn	0.05	0.05	0.04	0.06	0.04	0.06
Mg	3.08	3.09	3.15	3.13	3.00	3.10
Ca	1.85	1.87	1.88	1.88	1.85	1.84
Na_M	0.16	0.14	0.12	0.12	0.15	0.16
Na_A	0.23	0.23	0.22	0.29	0.22	0.24
K	0.15	0.15	0.13	0.16	0.17	0.15
A-site	0.37	0.38	0.36	0.45	0.39	0.39
Cl	0.02	0.02	0.02	0.03	0.02	0.02
OH* + F	1.98	1.98	1.99	1.97	1.98	1.98

Cation abundances were recalculated on the basis of 13 cations excluding Ca, Na, and K with Fe^{3+}/Fe^{2+} ratios calculated by charge balance (Cosca *et al.*, 1991).

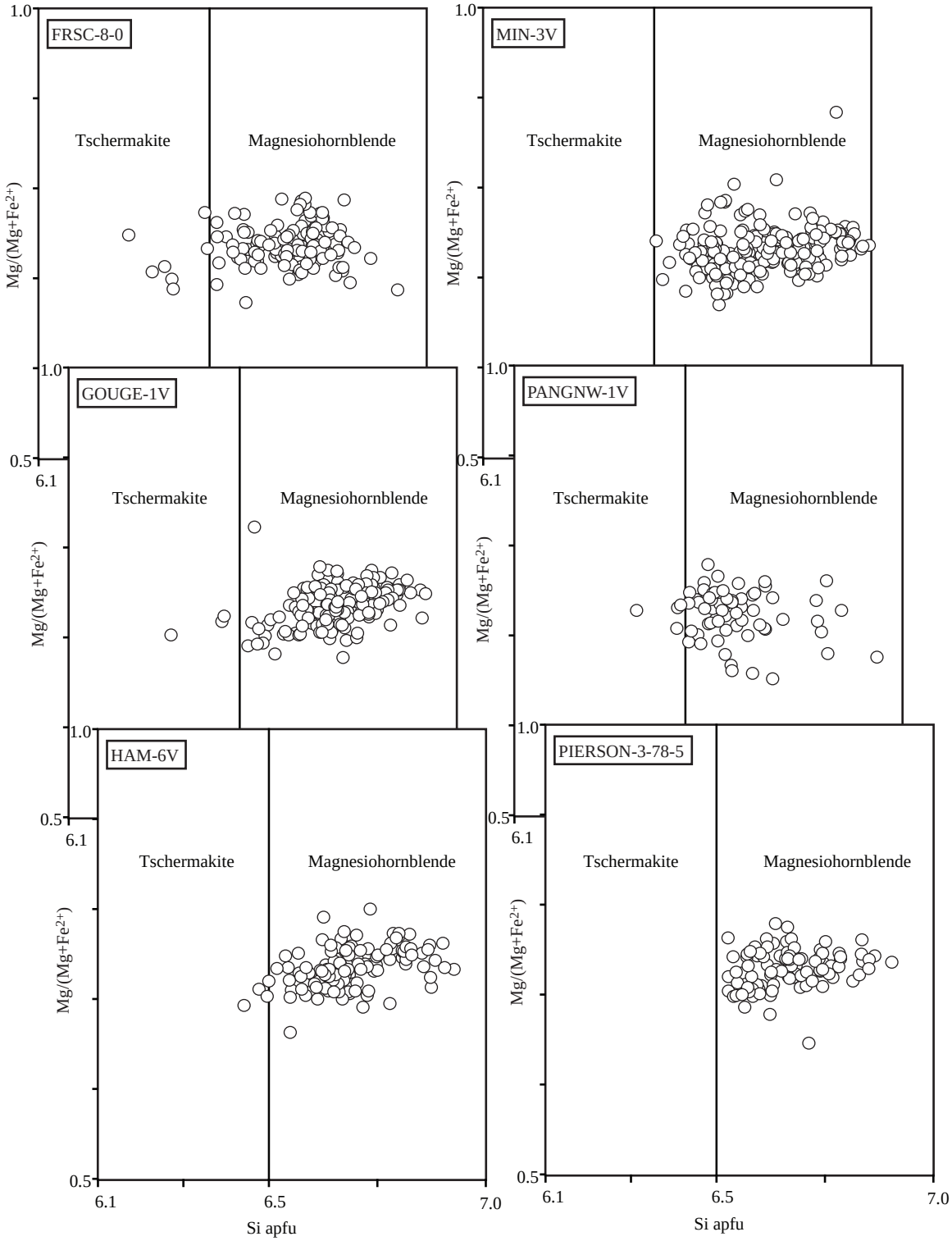

Fig.11. Hornblende classification diagrams (Leake *et al.*, 1997) showing most hornblendes in the Wah Wah Springs are magnesiohornblende $Ca^B \geq 1.50$; $(Na + K)^A < 0.50$; $Ca^A < 0.50$. Note there is little variation between samples.

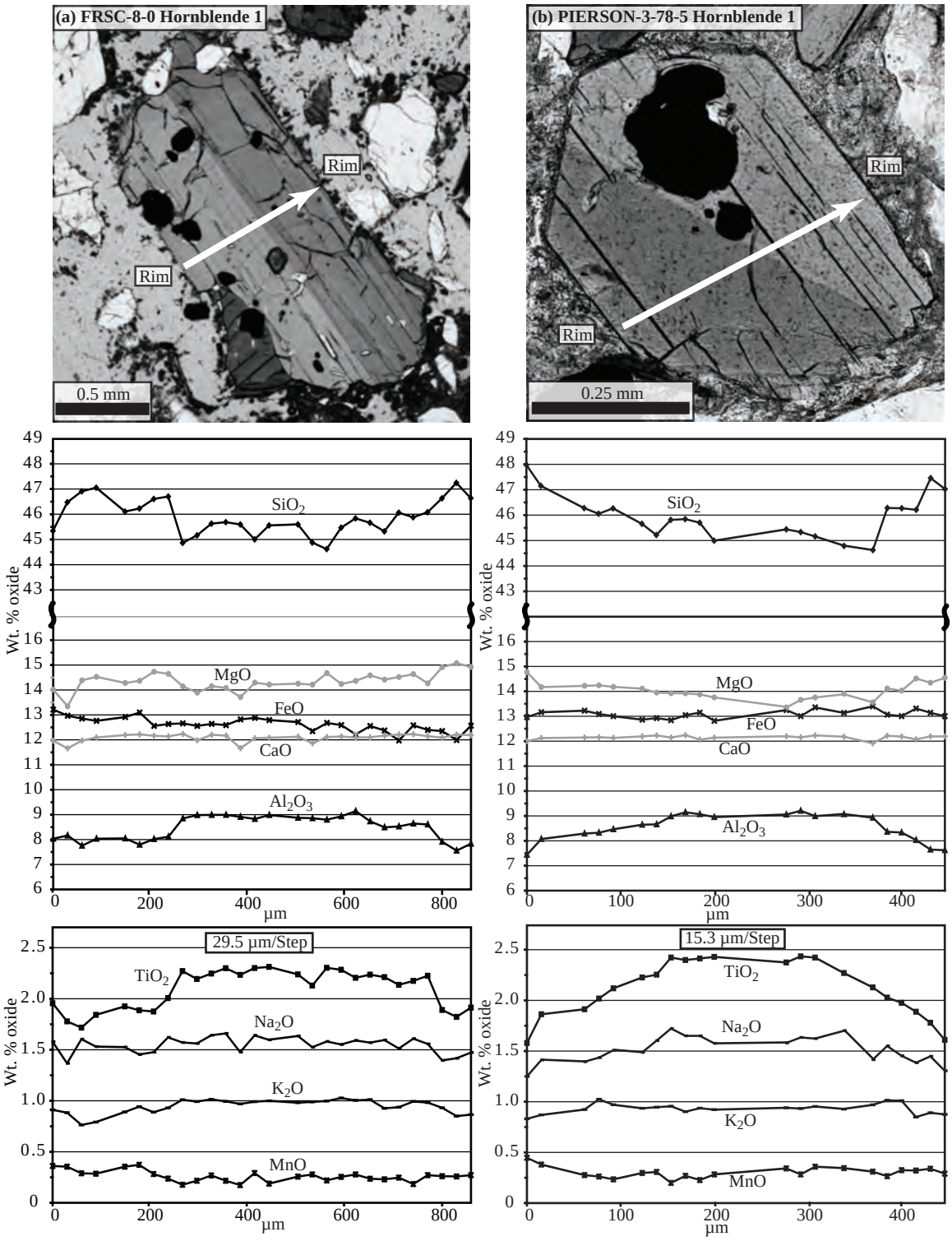

Fig.12. Hornblende traverses across four euhedral grains. The first three traverses show a decrease in Al_2O_3 and TiO_2 from core to rim indicating normal zonation and a cooling and crystallizing magma. The last traverse shows a flat profile pattern. (a) A hornblende from the FRSC-8-0 locality. (b) A hornblende grain from the PIERSON-3-78-5 locality.

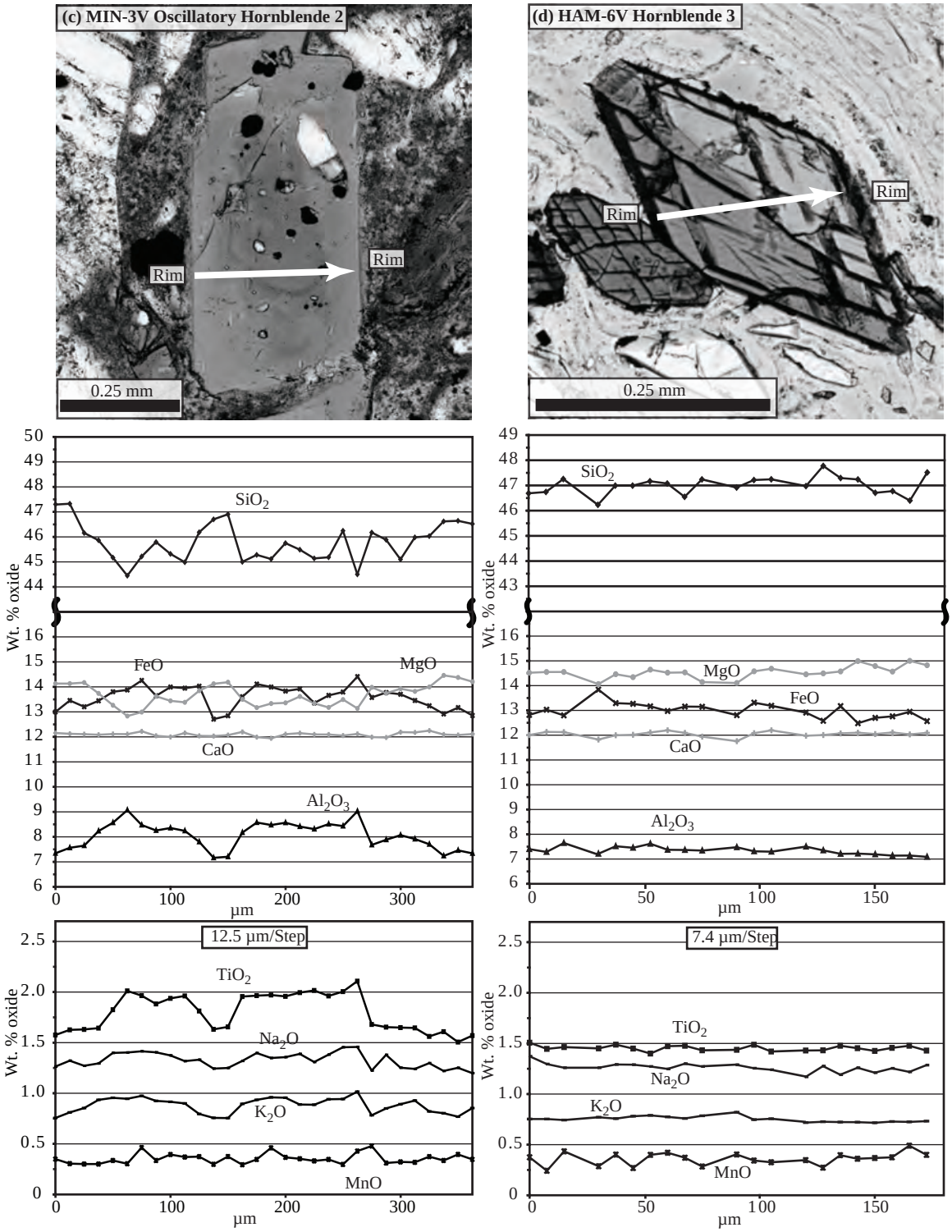

Fig. 12. (c) An oscillatory hornblende grain (MIN-3V) showing smaller scale oscillations within the larger overall normal zonation. (d) A hornblende grain from HAM-6V is unzoned and has a composition similar to rims on other grains.

system. This interpretation of the unzoned grains proves problematic, as there is no textural evidence that they formed at a different stage of magma development. Also, the unzoned grains show flat patterns up to 300 μm across, while the normally zoned grains only show compositions similar to the unzoned grains for small distances close to the rim. If there were two periods of crystal growth it could be expected that the normally zoned grains would have unzoned rims of similar sizes to the unzoned grains. A more probable interpretation is there is only one population of normally zoned grains and within this population a small number of grains showing flat patterns because of the way that were oriented and cut displaying only the rim of the crystal.

Biotite

Euhedral, tabular biotite phenocrysts range from 0.25-2.5 mm in length. Grains are often split along cleavage planes and bent as a result of differential compaction. Inclusions of hornblende, plagioclase, apatite, zircon, and opaque minerals are abundant (Fig. 7c). All major elements show little variation among the samples. For example Fe / (Fe+Mg) only ranges 0.36 – 0.40 in biotite from all of the samples (Table 5, Fig.6).

Quartz

Quartz appears as anhedral to subhedral grains with deep embayments and range from 0.25-1.75 mm across. They are ubiquitously fractured. Although resorbed grains are typical, one skeletal grain probably produced by rapid growth (Swanson & Fenn, 1986) was found in MIN-3V (Fig. 7d). Quartz was not found in HAM-6V or PIERSON-3-8-5.

Pyroxene

Both clinopyroxene and orthopyroxene were found as anhedral grains ranging from 0.25-1.5 mm across (Fig. 7e). Minor resorption along the margins of the grains is

Table 5. Representative chemical analyses of biotite from each locality in the Wah Wah Springs Tuff.

Sample:	FRSC-8-0	GOUGE-1V	HAM-6V	MIN-3V	PANGNW-1A	PIERSON-3-78-5
Sample No.:	B21	B39	B43	B55	B67	B111
wt. %						
SiO_2	37.90	35.82	37.73	37.53	35.76	37.83
TiO_2	4.82	4.43	4.64	4.89	5.07	4.92
Al_2O_3	13.81	14.25	13.77	14.34	13.74	13.82
FeO_{tot}	15.65	15.40	14.72	15.14	15.93	14.86
MnO	0.18	0.18	0.24	0.19	0.21	0.13
MgO	13.65	14.90	13.96	14.80	13.96	14.58
CaO	0.03	0.00	0.10	0.28	0.00	0.02
Na_2O	0.40	0.51	0.44	0.37	0.57	0.47
K_2O	8.87	9.56	9.30	7.64	9.30	9.00
BaO	0.54	0.39	0.43	0.36	0.97	0.68
Cl	0.16	0.15	0.13	0.13	0.10	0.13
Sum	95.96	95.56	95.42	95.64	95.60	96.40
H_2O*	3.87	3.86	3.85	3.95	3.83	3.91
Total	99.82	99.42	99.27	99.59	99.43	100.31
Fe/(Fe+Mg)	0.53	0.51	0.51	0.51	0.53	0.50
apfu						
Si	2.90	2.75	2.91	2.83	2.78	2.88
Al iv	1.10	1.25	1.09	1.17	1.22	1.12
Al vi	0.15	0.04	0.16	0.10	0.04	0.11
Ti	0.28	0.26	0.27	0.28	0.30	0.28
Fe_{tot}	1.00	0.99	0.95	0.95	1.04	0.95
Mn	0.01	0.01	0.02	0.01	0.01	0.01
Mg	1.56	1.70	1.60	1.66	1.62	1.65
Ca	0.00	0.00	0.01	0.02	0.00	0.00
Na	0.06	0.08	0.07	0.05	0.09	0.07
K	0.87	0.94	0.92	0.73	0.92	0.87
Ba	0.02	0.01	0.01	0.01	0.03	0.02
Cl	0.02	0.02	0.02	0.02	0.01	0.02
OH* + F	1.98	1.98	1.98	1.98	1.99	1.98

Biotite formulas were calculated by normalizing to 7 octahedral plus tetrahedral cations.

common. Clinopyroxene was found as cores in hornblende and as separate grains. In comparison, orthopyroxene was only found as cores in hornblende (Fig. 7f). Regardless of whether it was found in a core or separately, each phase is remarkably similar in composition (Table 6). Orthopyroxene is enstatite ($Wo_2\,Fs_{33}\,En_{65}$). Clinopyroxene compositions are mostly augite ($Wo_{45}\,Fs_{14}\,En_{41}$) but range to diopside (Fig. 13). Orthopyroxene was not found in MIN-3V or PANGNW-1V.

Accessory Minerals

Subhedral to anhedral Fe-Ti oxides range from 0.25-1.0 mm in size. These grains display resorption textures with embayments. Magnetite is very abundant but often displays trellis exsolution to ilmenite or is altered to hematite, making geothermometry difficult. Ilmenite grains are typically unaltered and very sparse compared to magnetite. Chemically both magnetites and ilmenites show some variation. X'usp in magnetite ranges from 0.12 to 0.19 and X'ilm in ilmenite ranges from 0.66 to 0.71 (Table 7). This may be due to either natural magmatic variation or the altered nature of the grains.

Apatite and zircon are often found as inclusions in most major phases. Rare apatite grains are also found separate within the groundmass.

THERMOBAROMETRY

An extensive set of geothermobarometers was used in an attempt to constrain temperature, pressure, and fO_2. Assessing the equilibrium of two or more phases in the system is essential to obtaining accurate temperature, pressure, and fO_2 estimates. Equilibrium can be more safely assumed with minerals that are in contact with each other. This can be difficult to determine in a pyroclastic system as the original location and textures of the phases will change dramatically upon eruption and emplacement.

Table 6. Representative chemical analyses of orthopyroxene and clinopyroxene from the Wah Wah Springs Tuff.

Sample:	FRSC-8-0		GOUGE-1V		HAM-6V		PIERSON-3-78-5	
Sample No.:	Cpx3	Opx4	Cpx21	Opx17	Cpx30	Opx30	Cpx79	Opx51
wt. %								
SiO_2	52.81	53.05	53.04	53.00	52.65	52.31	53.19	53.73
TiO_2	0.12	0.11	0.12	0.14	0.16	0.11	0.15	0.12
Al_2O_3	0.95	0.68	0.91	0.62	1.12	0.59	0.96	0.49
FeO_{tot}	8.50	20.41	8.34	21.03	8.71	20.67	7.71	19.44
MnO	0.62	1.26	0.57	1.32	0.62	1.21	0.57	1.22
MgO	14.47	23.75	14.60	23.21	14.77	23.99	15.09	23.99
Cr_2O_3	0.01	0.01	0.01	0.01	0.02	0.00	0.02	0.00
CaO	22.16	0.79	22.03	0.86	21.69	0.91	22.02	0.80
Na_2O	0.37	0.03	0.35	0.03	0.31	0.00	0.30	0.00
Total	100.01	100.08	99.97	100.19	100.04	99.78	100.00	99.80
Fe/(Fe+Mg)	0.18	0.33	0.24	0.34	0.25	0.33	0.22	0.30
Wo	44.84	1.54	44.66	1.69	43.80	1.75	44.51	1.61
En	40.74	65.14	41.21	63.84	41.53	64.98	42.43	66.35
Fs	14.42	33.32	14.13	34.48	14.67	33.27	13.06	32.04
apfu								
Na	0.03	0.00	0.03	0.00	0.02	0.00	0.02	0.00
Mg	0.81	1.31	0.81	1.29	0.82	1.33	0.84	1.32
Al	0.04	0.03	0.04	0.03	0.05	0.03	0.04	0.02
Si	1.97	1.97	1.98	1.97	1.96	1.95	1.97	1.99
Ca	0.89	0.03	0.88	0.03	0.87	0.04	0.88	0.03
Ti	0.00	0.00	0.00	0.00	0.00	0.00	0.00	0.00
Cr	0.00	0.00	0.00	0.00	0.00	0.00	0.00	0.00
Mn	0.02	0.04	0.02	0.04	0.02	0.04	0.02	0.04
Fe	0.27	0.63	0.26	0.65	0.27	0.65	0.24	0.60

Cations were calculated on the basis of 4 cations per formula unit with Fe^{3+}/Fe^{2+} calculated by charge balance (Morimoto *et al.*, 1988).

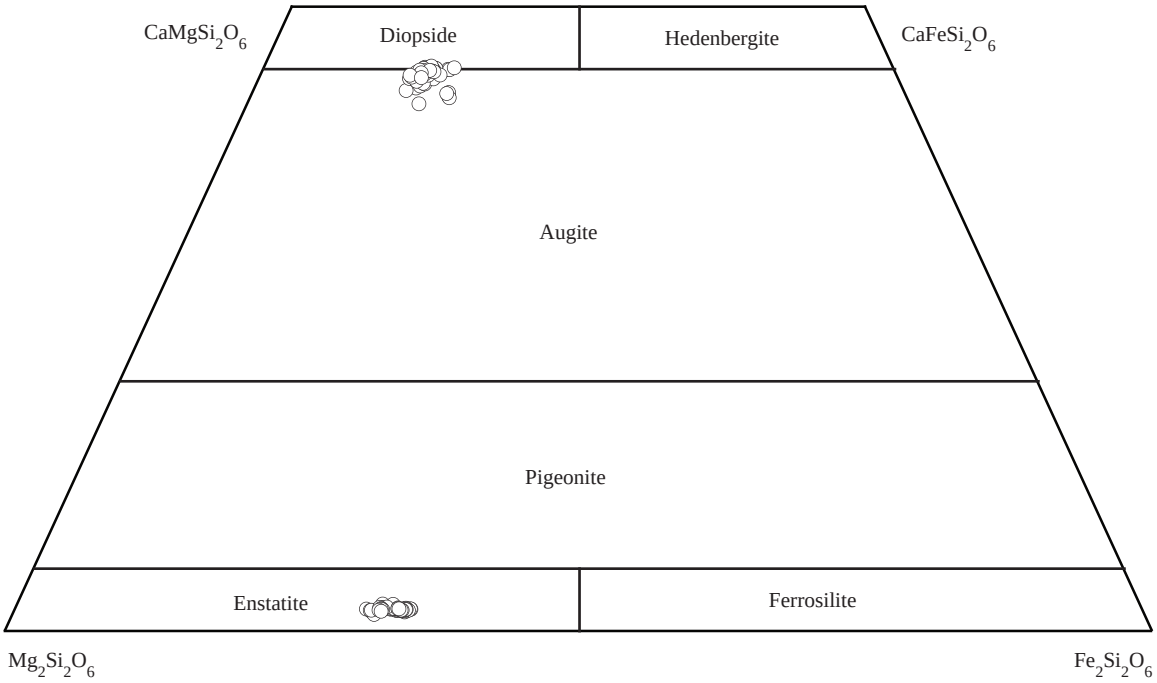

Fig. 13. Pyroxene compositions of the Wah Wah Springs Tuff. All orthopyroxenes are enstatite while clinopyroxenes range from augite to diopside. Orthopyroxene occurs only in cores of hornblende, and clinopyroxene grains are slightly resorbed.

Table 7. Representative chemical analyses for magnetite and ilmenite from the Wah Wah Springs Tuff.

Sample:	FRSC-8-0		GOUGE-1V		HAM-6V		MIN-3V	
Sample No.:	Mt7	I12	Mt20	I16	Mt50	I26	Mt58	I31
wt. %								
SiO_2	0.07	0.07	0.08	0.03	0.17	0.02	0.06	0.06
TiO_2	5.17	34.49	5.24	36.36	5.65	37.06	4.40	34.46
Al_2O_3	1.76	0.10	1.09	0.07	1.56	0.06	1.42	0.00
V_2O_3	0.65	1.37	0.61	1.28	0.59	1.35	0.53	1.36
Cr_2O_3	0.17	0.07	0.19	0.03	0.17	0.05	0.15	0.03
Re Fe_2O_3	54.19	33.12	56.55	29.07	54.32	27.16	58.32	33.27
Re FeO	33.60	28.55	33.82	29.69	34.40	30.37	34.17	28.26
MnO	0.63	0.52	0.62	0.63	0.62	0.65	0.64	0.81
MgO	0.98	1.33	1.16	1.58	1.12	1.55	0.86	1.30
ZnO		0.01		0.02		0.02		0.05
Nb_2O_5	0.27	0.31	0.15	0.38	0.28	0.40	0.38	0.34
Re Total	97.49	99.94	99.51	99.13	98.89	98.69	100.94	99.94
apfu								
X'usp	0.16	0.00	0.15	0.00	0.17	0.00	0.13	0.00
X'ilm	0.00	0.67	0.00	0.70	0.00	0.72	0.00	0.66
apfu								
Si	0.00	0.00	0.00	0.00	0.01	0.00	0.00	0.00
Ti	0.15	0.66	0.15	0.70	0.16	0.72	0.12	0.66
Al	0.08	0.00	0.05	0.00	0.07	0.00	0.06	0.00
V	0.02	0.03	0.02	0.03	0.02	0.03	0.02	0.03
Cr	0.01	0.00	0.01	0.00	0.01	0.00	0.00	0.00
Re Fe^{3+}	1.57	0.63	1.61	0.56	1.56	0.52	1.64	0.64
Re Fe^{2+}	1.08	0.61	1.07	0.63	1.09	0.65	1.07	0.60
Mn	0.02	0.01	0.02	0.01	0.02	0.01	0.02	0.02
Mg	0.06	0.05	0.07	0.06	0.06	0.06	0.05	0.05

The methods of Stormer (1983) and Ghiorso & Sack (1991) were used to calculate Fe-Ti oxide formulas.

Euhedral crystals bounded on all sides by "rational crystal faces" and surrounded by matrix or glass can usually be assumed to be equilibrium phases (Best, 2003). Unless otherwise noted in the discussion below, each set of minerals used for geothermobarometry was assumed to be in equilibrium, but anomalously low or high temperatures may indicate that this assumption is incorrect. The anhedral nature of some phenocrysts, especially the rounded clinopyroxenes and embayed quartz, may also indicate disequilibrium at some pre-eruptive state. Some of the geothermobarometers produced reasonable temperatures, pressures, and fO_2 while others produced anomalously low or high values.

In order to specifically constrain temperature and pressure shortly before eruption, phenocrysts textures and chemical variation across a grain were used to differentiate cores versus rims in hornblende and plagioclase. A comparison of the intensive parameters from core to rim is also the most decisive evidence for whether or not there was a re-heating event. Each of the geothermobarometers used for this investigation and the appropriate parameters calculated by each one (Table 8) will be discussed mineral by mineral below.

Plagioclase

The Wah Wah Springs does not contain sanidine, ruling out any use of the numerous two feldspar thermometers. One thermobarometer uses plagioclase in equilibrium with melt (Putirka, 2005). For this method each plagioclase rim analysis was paired with each glass analysis for a given sample. For the Wah Wah Springs this thermobarometer produced fairly high temperatures (808 - 845°C, avg. 826 ± 19°C) and highly variable pressures (1.3 – 6.4 kb, avg. 3.5 ± 2.4 kb), (Table 8).

Table 8. Summary of geothermobaromety for the Wah Wah Springs Tuff.

Sample:		FRSC-8-0	GOUGE-1V	HAM-6V	MIN-3V	PANGNW-1A	PIERSON 3-78-5
Phases							
Temperature							
Plagioclase + Melt	Putirka (2005)	845 ± 10°	836 ± 10°	839 ± 9°	825 ± 4°	808 ± 14°	827 ± 15°
Hornblende (with or without qtz)	Holland & Blundy (1994)	781 ± 16°	793 ± 17°	797 ± 21°	773 ± 10°	793 ± 27°	797 ± 14°
Hornblende (requiring qtz)	Holland & Blundy (1994)	812 ± 26°	821 ± 27°	N/A	812 ± 21°	834 ± 46°	N/A
Fe-Ti Oxides	Anderson *et al.* (1993), (QUILF)	800 ± 8°	748 ± 43°	787 ± 16°	777 ± 25°	822 ± 2°	820 ± 3°
Fe-Ti Oxides + Pyroxenes	Anderson *et al.* (1993), (QUILF)	742	713	714	726	719	720
Fe-Ti Oxides	Sauerzapf *et al.* (2008)	826 ± 9°	762 ± 48°	811 ± 22°	786 ± 18°	857°	856 ± 2°
Fe-Ti Oxides	Ghiorso & Evans (in press)	773 ± 9°	710 ± 35°	756 ± 25°	718 ± 43°	805 ± 1°	802 ± 3°
Two Pyroxenes	Anderson *et al.* (1993), (QUILF)	856 ± 22°	859 ± 15°	875 ± 16°	N/A	N/A	859 ± 15°
Cpx + Melt	Putirka *et al.* (2003)	808 ± 33°	764 ± 28°	750 ± 34°	780 ± 6°	738 ± 32°	786 ± 10°
Biotite	Luhr *et al.* (1985)	818 ± 11°	833 ± 18°	851 ± 8°	818 ± 29°	837 ± 14°	850 ± 16°
Biotite + Melt	Righter & Carmichael (1996)	850 ± 2°	868 ± 3°	864 ± 2°	864 ± 4°	860 ± 2°	865 ± 2°
Biotite	Henry (2005)	766 ± 4°	772 ± 5°	777 ± 4°	768 ± 8°	774 ± 3°	772 ± 5°
Pressure							
Hornblende	Johnson & Rutherford (1989b)	2.3 ± 0.2	2.1 ± 0.3	2.2 ± 0.4	2.0 ± 0.4	2.5 ± 0.5	2.2 ± 0.3
Hornblende	Anderson & Smith (1995)	1.9 ± 0.2	1.7 ± 0.3	1.8 ± 0.4	1.6 ± 0.4	2.1 ± 0.5	1.8 ± 0.3
Pyroxene + melt	Putirka *et al.* (2003)	10.6 ± 1.2	7.8 ± 1.5	7.0 ± 2.0	10.1 ± 1.0	10.1 ± 4.2	9.8 ± 1.1
Plagioclase + melt	Putirka (2005)	6.4 ± 0.9	5.0 ± 0.8	4.7 ± 0.7	4.8 ± 0.2	1.3 ± 2.4	4.1 ± 1.3
fO_2							
Fe-Ti Oxides	Anderson *et al.* (1993), (QUILF)	2.9 ± 0.1	3.1 ± 0.1	2.9 ± 0.1	3.1 ± 0.2	2.7 ± <0.01	2.7 ± 0.03
Fe-Ti Oxides	Sauerzapf *et al.* (2008)	2.9 ± 0.1	3.2 ± 0.3	2.9 ± 0.1	3.3 ± 0.1	2.7	2.7 ± 0.01
Fe-Ti Oxides	Ghiorso and Evans (in press)	2.1 ± 0.02	2.2 ± 0.1	2.1 ± 0.1	2.2 ± 0.1	2.00 ± <0.01	2.00 ± <0.01

The mean temperature (°C), pressure (kb), and fO_2 (Δ QFM) is listed for each sample. Those geothermobarometers using hornblende plus plagioclase and plagioclase plus melt represent intensive parameters of the rims only. Errors are one standard deviation.

Hornblende

Holland & Blundy (1994) use plagioclase in conjunction with amphibole in order to constrain temperature. To ensure that temperatures shortly before eruption were obtained, rim compositions from hornblende were matched with rim compositions of plagioclase. One thermometer that does not require quartz in the phase assemblage gives reasonable temperatures (773 - 797°C, avg. 791 ± 20°C). The other method that does require quartz gives higher temperatures (812 - 834°C, avg. 818 ± 29°C).

The Al-in-hornblende barometer has been calibrated and used by several investigators to constrain magma pressure. Empirical models to constrain pressure were first established (Hammerstrom & Zen, 1986; Hollister *et al.*, 1987). Later experimental studies in controlled settings further constrained the effect of pressure on Al in hornblende and confirmed that Al-in-hornblende could be a viable barometer (Johnson & Rutherford, 1989a, b; Schmidt, 1992). However, others have indicated that this barometer is not without its drawbacks, and it may produce erroneous results as increasing temperature and decreasing oxygen fugacity can also increase Al concentration in hornblende and produce higher pressure estimates (Blundy & Holland, 1990; Anderson & Smith, 1995). For this barometer to be effective, a specific phase assemblage must be present in the rock. The presence of quartz, sanidine, plagioclase, hornblende, biotite, ilmenite, magnetite, and titanite indicate that the effects of temperature and oxygen fugacity on the Al concentration in hornblende are minimized. The Wah Wah Springs Tuff does not contain titanite or sanidine. However, Johnson & Rutherford (1989b) indicate that the lack of sphene may be negligible, and that if the concentration of K_2O in the melt is around 5 wt. % the barometer can still be used as it is nearly sanidine

saturated. Glass in the Wah Wah Springs has a mean K_2O concentration of 5.04 ± 0.48 wt. % thus allowing for the use of this method.

When used on the Wah Wah Springs, the Johnson & Rutherford (1989b) barometer appears to produce reasonable results (2.0 – 2.5 kb, avg. 2.2 kb). The Anderson & Smith (1995) barometer produces slightly lower pressures (1.6 – 2.1 kb, avg. 1.8 kb) because of a temperature correction. Even though these methods produce different results, each one predicts pressures in the same increasing order from lowest to highest (Table 8).

Fe-Ti Oxides

Several geothermometers use the compositions of co-existing Fe-Ti oxides (magnetite and ilmenite) to constrain both eruption temperatures and fO_2. Because Fe-Ti oxides re-equilibrate quickly, temperatures and fO_2 estimates are useful measures of conditions shortly before eruption. A test of equilibrium has been established based on Mg/Mn ratios in these two minerals (Bacon & Hirschmann, 1988). In the Wah Wah Springs, each magnetite analysis was paired with each ilmenite analysis for a given sample to assess equilibrium. Only the pairs that had Mg/Mn ratios consistent with equilibrium were used. This produced a total of 397 pairs; however, this number is not split proportionally among the samples. For instance, FRSC-8-0 accounts for 177 of those pairs while PANGNW-1V only produced two suitable pairs. The temperature and fO_2 reported below are the means of all the pairs from each sample.

The computer program QUILF (Anderson *et al.,* 1993) assesses equilibria and also calculates temperature and fO_2 for Fe-Ti oxides. Using this method for the Wah Wah Springs Tuff produced reasonable mean temperatures, though there was a large range of

average temperatures for each sample (748 – 822°C, avg. of all calculated temperatures 788 ± 30°C). QUILF produced fO_2 estimates slightly higher than those estimated by Ghiorso & Evans (in press), (2.7 – 3.1 ΔQFM, avg. 2.9 ± 0.3 ΔQFM), (Fig. 14). In QUILF, the Fe-Ti oxide compositions can be combined with pyroxene compositions to further constrain the results. When this is done for the Wah Wah Springs, the temperature estimates have a narrower range, and lower values (713 - 742°C) are produced (Table 8). This indicates that the pyroxenes and Fe-Ti oxides may not be in equilibrium with each other. The calibration proposed by Sauerzapf *et al.* (2008) produced slightly higher temperatures than the other oxide thermometers and had a largest range overall (752 – 856°C, avg. 804 ± 40°C) but produced fO_2 estimates very similar to QUILF (2.7 – 3.3 ΔQFM, avg. 3.0 ± 0.3 ΔQFM), (Fig. 14). The slightly higher temperatures produced by this thermometer may be because the number of experiments used in the calibration at temperatures below 800°C was not as large as for higher temperatures. The Wah Wah Springs also appears to have a slightly higher fO_2 (~3.0 ΔQFM) than what was used to calibrate the thermometer (~ -4.6 to 1.4 ΔQFM). Ghiorso & Evans (in press) latest geothermometer based on the composition of Fe-Ti oxides produces viable results for temperature (Table 8). However, there is a large range of calculated temperatures among samples and the mean temperature is lower than most other geothermometers (710 - 805°C, avg. 759 ± 35°C). The fO_2 produced by this technique is also reasonable and similar among samples (2.0 – 2.2 ΔQFM, avg. 2.1 ± 0.2 ΔQFM), (Fig. 14).

Pyroxene

Two methods involving pyroxene were used to assess temperature and pressure. The first method uses the composition of orthopyroxene and clinopyroxene in QUILF

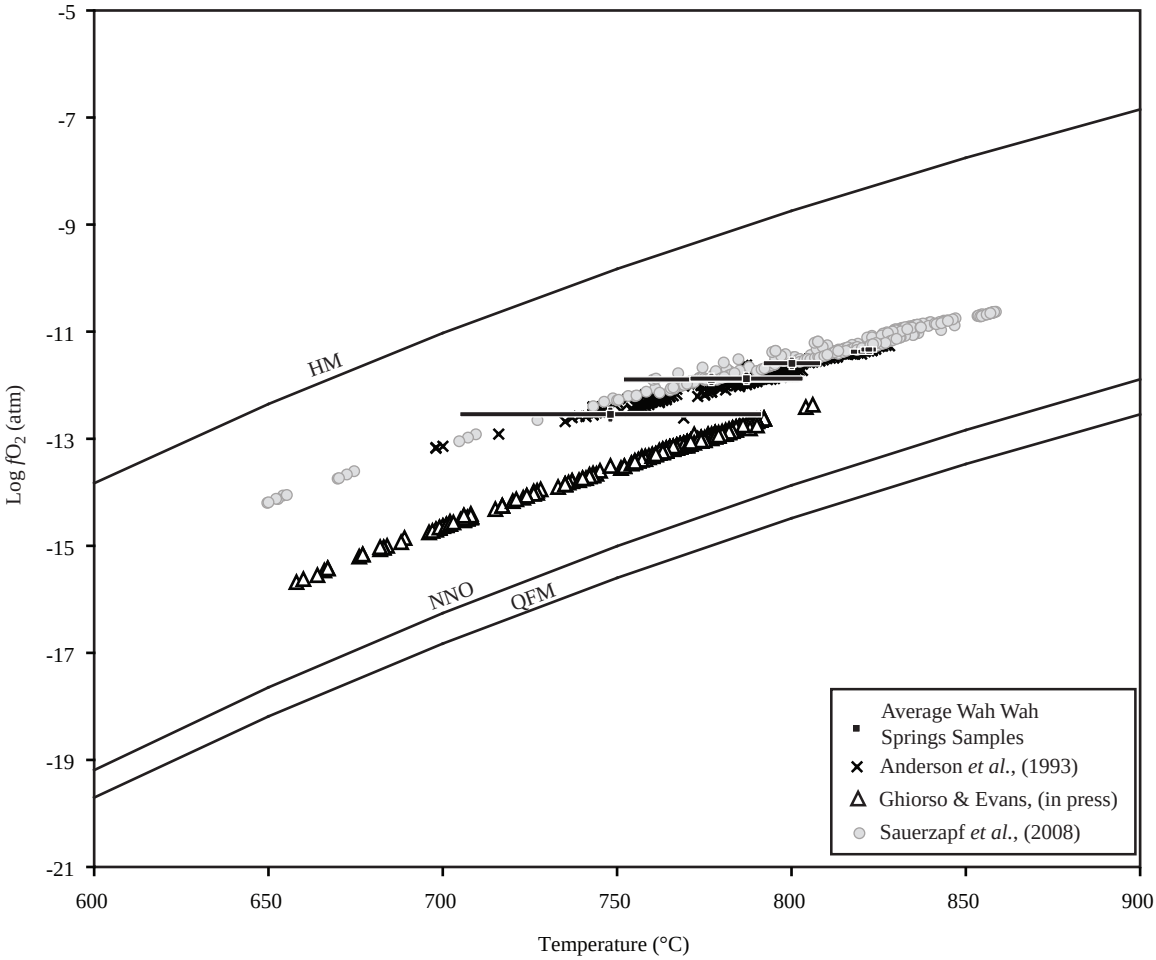

Fig. 14. Log fO_2 versus temperature for each oxybarometer used in this study. Each symbol represents a single pair of analyses that passed the Mg/Mn test for equilibrium (Bacon & Hirchmann, 1988). Average Wah Wah Springs samples represent the average temperatures and fO_2 for each pair calculated in the Anderson *et al*. (1993) oxybarometer. Error bars represent one standard deviation.

(Anderson *et al.*, 2003) to determine temperature. Both clinopyroxene and orthopyroxene compositions in the Wah Wah Springs Tuff were very similar between the samples. Each clinopyroxene analysis was paired with each orthopyroxene analysis within each sample, and the average was calculated. This method produced higher temperatures than any of the other techniques (856- 875°C, avg. 862 ± 19°C). Comparing these higher than expected temperatures with the lower than expected temperatures of pyroxenes combined with Fe-Ti oxides indicates that the pyroxenes are out of equilibrium with the rest of the system. The rounded and resorbed nature of the clinopyroxenes and the fact that orthopyroxenes are found only in the cores of hornblendes also support this claim. Additionally, MIN-3V and PANGNW-1V did not have any orthopyroxene.

The other method involves equilibrium between clinopyroxene and melt (Putirka *et al.*, 2003). Again, an average temperature was calculated by pairing each clinopyroxene analysis with each glass analysis for a given sample. Compared to others this thermometer produced relatively low temperatures on average and had a wide range (738 – 808°C, avg. 762 ± 37°C). The clinopyroxene-melt barometer also produced much higher pressure estimates (7.0 – 10.6 kb) than the Al-in-hornblende barometer (Johnson & Rutherford, 1989a). This thermobarometer was calibrated at temperatures that may be slightly higher than the Wah Wah Springs (850° to 1430° C). Also, the thermobarometer appears to be slightly sensitive to Na_2O concentration which may have changed in the Wah Wah Springs glass due to alteration.

Biotite

Biotite compositions can also be used to assess temperature. Luhr *et al.* (1985) proposed a geothermometer based on natural biotite compositions and temperatures

calculated from coexisting Fe-Ti oxides. The equation involves total Fe and Ti concentrations in biotite and produced relatively high estimate of temperature (818 – 851°C, avg. 839 ± 23°C). Righter & Carmichael (1996) formulated a biotite geothermometer based on Ti concentrations in glass and biotite. It also produced very high temperatures (850 – 868°C, avg. 863 ± 8°C). Henry (2005) uses Ti, Mg, and Fe concentrations in biotite. Although this thermometer was calibrated using peraluminous graphitic metapelites with rutile at higher pressures (~4 to 6 kb) than presumed for the Wah Wah Springs, it produced temperatures (766 – 777°C, avg. 770 ± 7°C) that lie near the center of the other temperature estimates (Table 8). Each biotite thermometer produces a small range of temperatures indicating that biotite may re-equilibrate quickly to changing magmatic temperatures.

Summary of Thermobarometry

With such a wide range of results for intensive parameters among the set of thermobarometers it is beneficial to summarize those that produce the most ideal results for the Wah Wah Springs Tuff, and how those ideal conditions were estimated. Using the phase diagram for the compositionally similar Fish Canyon Tuff (Johnson & Rutherford, 1989a), the probable temperature range for the Wah Wah Springs magma was between 775°C - 800°C at pressures between 2.0 – 2.5 kb (Fig. 15). Under these conditions the phase assemblage of quartz, plagioclase, biotite, hornblende and Fe-Ti oxides is stable as is typical of the Wah Wah Springs. Quartz becomes unstable at the higher temperatures and pressures. The two samples that do not have quartz (HAM-6V and PIERSON-3-78-5) often have the highest temperatures in each of the thermometers used. The conditions

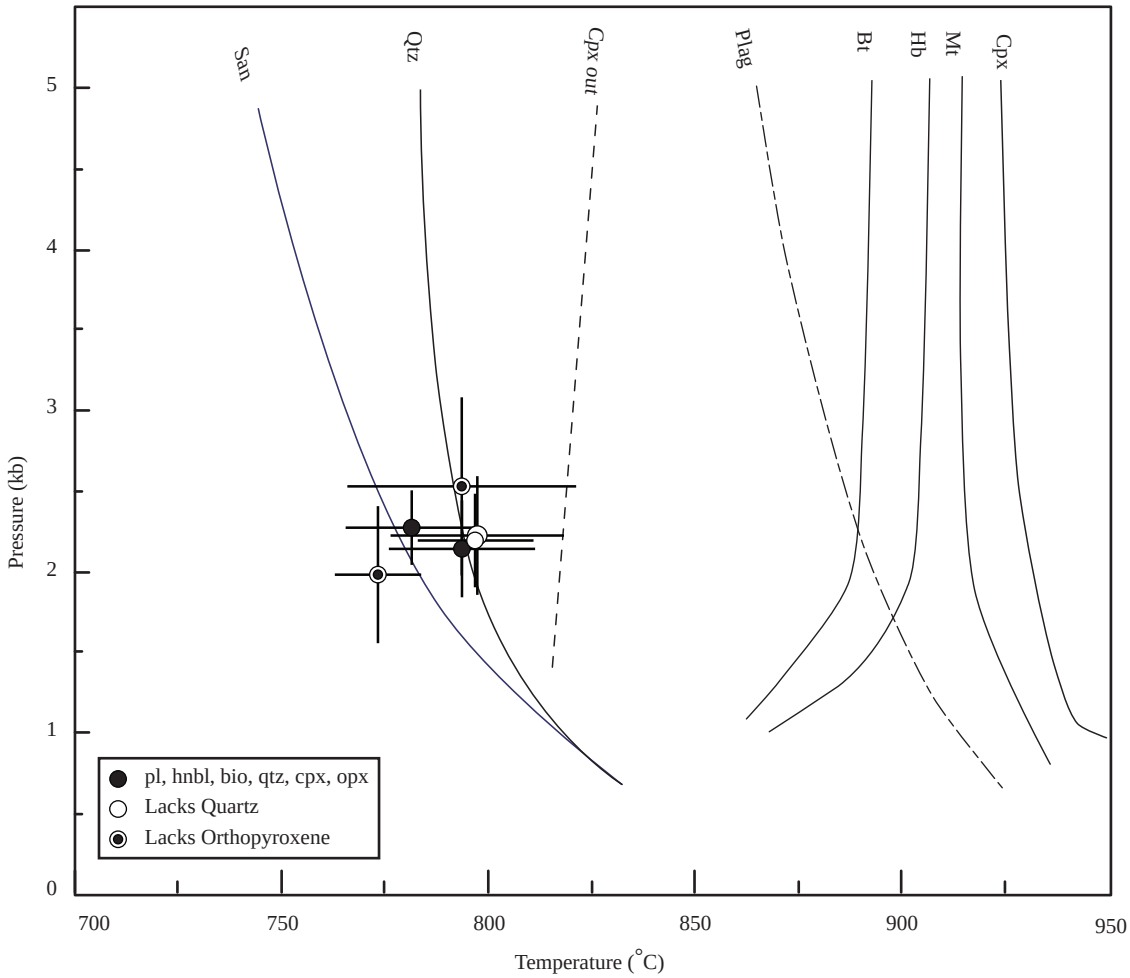

Fig. 15. Phase diagram from experiments on the Fish Canyon Tuff (Johnson & Rutherford, 1989a) with 0.5 X_{H2O} in fluid. Pressures and temperatures for the Wah Wah Springs Tuff are estimated from the Al-in-hornblende barometer (Johnson & Rutherford, 1989b) and hornblende-plagioclase thermometer not requiring quartz (Holland & Blundy, 1994). Rim compositions of plagioclase and hornblende were used and the average temperature and pressure for each sample is shown. Circles represent the observed phase assemblage for each sample. Error bars represent one standard deviation.

for the Wah Wah Springs magma fall below the clinopyroxene-out line which is consistent with evidence for clinopyroxene being out of equilibrium in the system.

Several of the thermometers yield temperature estimates that fall within the preferred temperature range for the Wah Wah Springs. Of these, the hornblende-plagioclase thermometer with or without quartz (Holland & Blundy, 1994) and QUILF using Fe-Ti oxides only (Anderson *et al.*, 1993), appear to be the most consistent with the experiments and phase assemblage present and produce almost identical average temperatures. The biotite (Henry, 2005) and Fe-Ti oxide (Sauerzapf *et al.*, 2008) thermometers produce results somewhat close to the expected estimates. The Al-in-hornblende barometer (Johnson & Rutherford, 1989a) produced the expected pressure estimates. Anderson *et al.* (1993) (oxides only) and Sauerzapf *et al.* (2008) produce similar estimates of fO_2 for $X_{H2O} = 0.5$.

DISCUSSION

Comparison to Other Monotonous Intermediates

Several studies of monotonous intermediate ignimbrites exist. Of these, the Fish Canyon Tuff (Bachmann *et al.*, 2002; Johnson & Rutherford, 1989a,b; Whitney & Stormer, 1985), the Lund Tuff (Maughan *et al.*, 2002), and those in the central Andes (Lindsay *et al.*, 2001; de Silva *et al.*, 1994; de Silva, 1989; Francis *et al.*, 1989) are considered below for comparison to the Wah Wah Springs Tuff.

Modally, the Wah Wah Springs Tuff is similar to other monotonous intermediates. The description monotonous comes into question because of the significant variation in bulk rock composition and modal differences between samples (Fig. 4 and 5). However, mineral compositions appear to be fairly uniform between

samples. Despite the similarities in modal proportions among the monotonous intermediates ignimbrites, there are key differences. The Wah Wah Springs does not contain sanidine or titanite while minor amounts of these phases are reported in the Lund Tuff and in some of the Central Andes deposits. However, sanidine is abundant in the Fish Canyon Tuff. The Central Andes deposits and the Wah Wah Springs do contain small amounts of clinopyroxene while it is absent in the Lund and Fish Canyon Tuff. Quartz is impersistent in the Wah Wah Springs Tuff but found in each of the other deposits. The lack of sanidine and sphene, the absence of quartz in some samples, and the general presence of clinopyroxene is consistent with the higher temperature of the Wah Wah Springs and Central Andes tuffs compared to the Fish Canyon and Lund. The absence of quartz in some samples in the Wah Wah Springs may be due to a small sampling bias combined with the small percentage the phase.

With respect to the Fish Canyon Tuff phase diagram, the estimated intensive parameters of the Wah Wah Springs Tuff are between 775°C – 800°C, 2.0 – 2.5 kb, and 2 – 3 ΔQFM. The intensive parameters of the Lund Tuff (740° – 800°C, ~2.5 kb, and ~2.7 ΔQFM), (Maughan *et al.*, 2002) and the central Andes ignimbrites (770° – 790°C, 1.1 – 3.3 kb, and ~3 ΔQFM), (Lindsay *et al.*, 2001; de Silva *et al.*, 1994; Francis *et al.*, 1989) are similar to the Wah Wah Springs Tuff. The Fish Canyon Tuff yields slightly lower temperatures (760 ± 30°C) but similar pressures and fO_2 are estimated (2.4 kb and ~3 ΔQFM, respectively) (Johnson & Rutherford, 1989a).

Bachmann *et al.* (2002) found a low-Al "population" within the cores of some hornblendes in the Fish Canyon Tuff. This population is key evidence for the rejuvenation model as it indicates the cores of these grains crystallized or re-equilibrated

at lower temperature (~715°C). These cores also have low concentrations of Ti. The grains have high-Al (and high-Ti) rims inferred to be the result of higher temperatures. No similarly low-Al hornblendes were found in the Wah Wah Springs Tuff (Fig. 16). This indicates that unlike the Fish Canyon there is no preserved evidence that the Wah Wah Springs magma ever cooled to a temperature low enough to produce this low-Al hornblende and did not experience thermal rejuvenation to remelt and erupt. Plagioclase is normally zoned, like hornblende, with an overall decrease in An content from cores to rims, also indicating a decrease in temperature. Pyroxene geothermometry may also indicate the magma was cooling before eruption. Experiments on the Fish Canyon Tuff (Johnson & Rutherford, 1989a) indicate that clinopyroxene is stable at temperatures slightly higher than estimates for Wah Wah Springs Tuff. The two pyroxene thermometer (Anderson *et al.*, 1993) produced the highest temperature estimates of any of the thermometers used in this study (Table 8). These estimates may be preserved temperatures from an earlier stage in the evolution of the magma prior to eruption. The textural character of the clinopyroxenes supports this conclusion.

Open System Behavior?

Nusbaum (1990) makes a case for open system behavior and magma hybridization in the Wah Wah Springs Tuff by pointing to four observations: (1) modestly zoned phenocrysts; (2) two distinct clinopyroxene populations; (3) resorbed plagioclase, biotite, and hornblende; and (4) reverse zoning in plagioclase within pumice lapilli. Nusbaum's (1990) model for hybridization involves mixing of a highly evolved rhyolitic melt with more mafic magma. This model is used to account for the presence of the high SiO_2 rhyolite glass in the tuff as well as the four observations listed above.

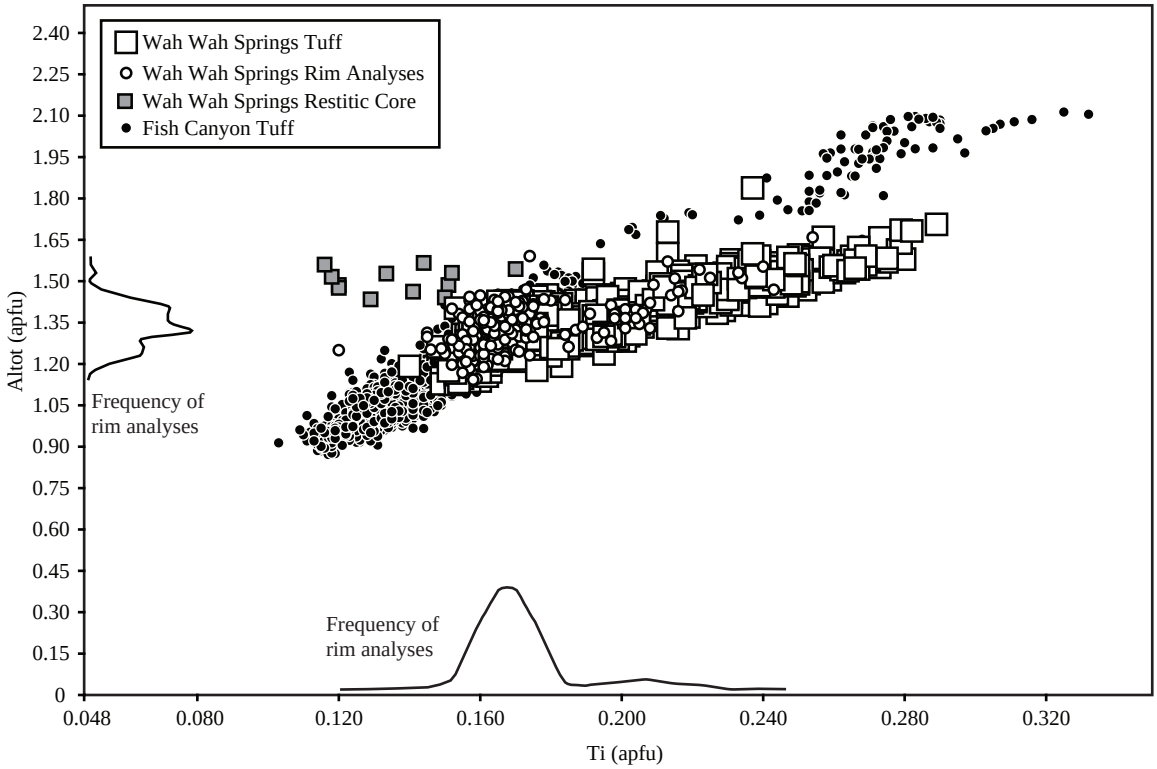

Fig. 16. Al variation in the Wah Wah Springs Tuff and the Fish Canyon Tuff. Note the Wah Wah Springs lacks a low-Al population. Rim compositions show little variation. Histograms along each axis show the frequency of the rim analyses. Restitic core samples are from the MIN-3V Oscillitory Hornblende 4 grain (Appendix D).

While several observations made in Nusbaum (1990) are similar to those made in this study there are some differences which shed light on the main conclusions of Nusbaum (1990).

First, experiments with the Fish Canyon Tuff (Johnson & Rutherford, 1989a) produced compositions of hornblende and high SiO_2 rhyolite glass very similar to the Wah Wah Springs Tuff at temperatures of 780°C (Fig. 17). The Lund Tuff (Maughan *et al.*, 2002) and ignimbrites from the central Andes (Lindsay *et al.*, 2001; de Silva *et al.*, 1994) also contain high-silica glass and similar phenocrysts compositions as the Wah Wah Springs Tuff. Nusbaum (1990) argues that the Wah Wah Springs glass composition is higher in SiO_2 and CaO and that the temperature is higher than in the Fish Canyon magma. Consequently, the glass cannot be in equilibrium with the phenocrysts according to the Fish Canyon experiments. However, this obstacle is minimized because of the lower temperatures calculated by the new Fe-Ti oxide and hornblende-plagioclase thermometers and the larger range of glass compositions collected in this study. As a result of these new data, we conclude glass in the Wah Wah Springs Tuff is similar to that in the Fish Canyon Tuff, but the former has a slightly larger range of compositions and the magma a higher temperature. The new glass compositions from this study plot along the $XH_2O=0.5$ line produced by the Fish Canyon experiments showing that the glass is in equilibrium with the phenocrysts at this concentration of water and at 2 kb of pressure (Fig. 17).

The modest normal zonation of plagioclase and hornblende found in this study and by Nusbaum (1990) are similar. Conversely, reverse zonation of plagioclase was not observed in this study. Nusbaum (1990) identified two populations of clinopyroxene

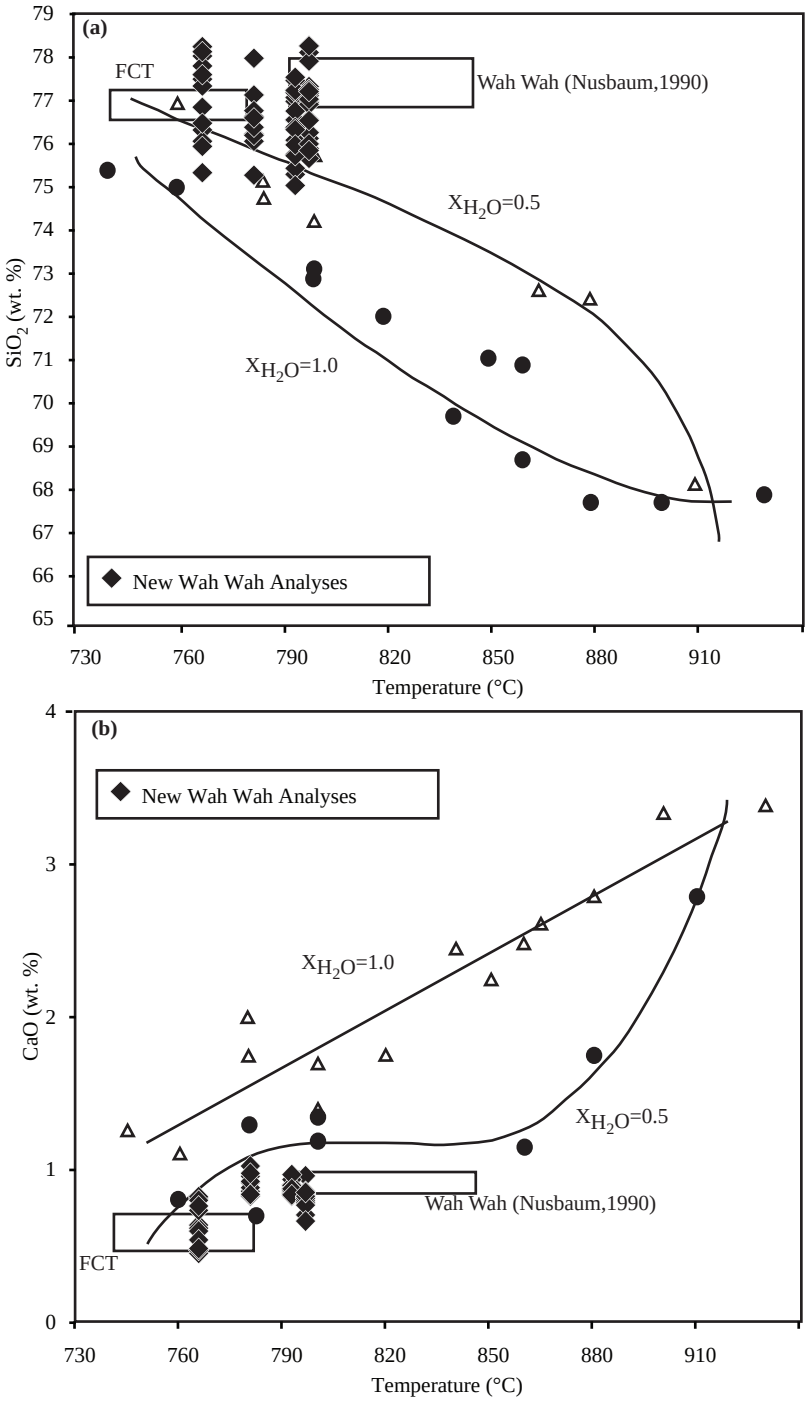

Fig. 17. Glass compositions as a function of temperature from the Fish Canyon Tuff experiments of Johnson & Rutherford (1989a). Both diagrams are at 2 kb and show data from the Fish Canyon (triangles and closed circles), and Wah Wah Springs. Both old data (from Nusbaum (1990)) and new data from this study are shown here. Both diagrams suggest that rhyolite glass from the Wah Wah was in equilibrium with the phenocrysts at low X_{H_20}. (a) SiO_2 vs temperature. (b) CaO vs temperature

based on textural and chemical evidence. One group was found as separate euhedral grains ($Wo_{48}En_{42}Fs_{10}$) while the second was found in the cores of hornblendes and had a slightly different composition ($Wo_{45}En_{44}Fs_{11}$). Separate grains were identified in this study, though not euhedral, as well as grains in the cores of hornblendes. However, there is such little variation in clinopyroxene compositions that we conclude they are actually one population (Fig. 13). Slightly resorbed phenocrysts of plagioclase were also observed in this study, but resorption of biotite and hornblende was not seen. Along the margins of some biotite and hornblende grains there are irregular surfaces that appear to be the result of late stage growth or fracturing upon eruption rather than resorption.

If a high-silica rhyolitic melt had been added to the magma system strong normal zonation of phenocrysts from the more mafic magma would result, and phenocrysts in the high-silica melt would show reverse zonation. Finally, it is difficult to conceive how approximately 1500 km^3 of highly evolved silica melt could "efficiently" mix with a more mafic magma to create the observed Wah Wah Springs Tuff.

CONCLUSIONS

The Wah Wah Springs Tuff is a crystal-rich, "monotonous intermediate" ignimbrite with intermediate concentrations of silica (~63 to ~70 wt. %) and a major phase assemblage of plagioclase, hornblende, biotite, quartz, minor clinopyroxene, orthopyroxene, Fe-Ti oxides, apatite, and zircon. The Wah Wah Springs is modally and compositionally similar to other monotonous intermediates, with a few exceptions. Phase diagrams produced from experiments on the similar Fish Canyon Tuff indicate the magma equilibrated between 775°C – 800°C. The hornblende-plagioclase thermometer of Holland & Blundy (1994) and the Fe-Ti oxides thermometer of Anderson *et al.* (1993)

most consistently yield the temperatures within this range. The Al-in-hornblende geobarometer of Johnson & Rutherford (1989b) indicates pressures between 2.0 and 2.5 kb. The oxybarometer of Anderson *et al.* (1993) indicate the fO_2 of Wah Wah Springs magma was 2 – 3 log units above the quartz-fayalite-magnetite buffer.

These conditions in the parent magma for the Wah Wah Springs differ from interpretations of mineral compositions in the Fish Canyon Tuff by Bachman *et al.* (2002) who proposed compelling evidence that the near solidus magma body was "rejuvenated" or reheated prior to eruption. In contrast, the extensive data set used for this study indicates that the magma which erupted to form the Wah Wah Springs Tuff does not preserve evidence for the magma body undergoing multiple reheating events that ultimately led to a large volume of eruptible magma

Rather, the Wah Wah magma appears to have been cooling and crystallizing with only minor oscillations of intensive parameters until it erupted. This is evidenced by the normal zonation of hornblende and plagioclase showing a decrease in temperature from core to rim. Also, temperature estimates using pyroxenes show higher, and presumably, relict temperatures since they are resorbed and out of equilibrium in the system. Similar mineral compositions and intensive parameters between samples indicate there was little systematic zonation in the magma chamber. The magma appears to have had a composition, pressure, temperature, and fO_2 where sanidine is absent, clinopyroxene was nearly all resorbed, and quartz is impersistent.

This raises questions, which of these two styles of pre-eruptive behavior is most common? Which style is exceptional in magma systems and more specifically, in monotonous intermediates? With so many similarities between the various monotonous

intermediate ignimbrites why is evidence of rejuvenation preserved in some but evidence of crystallizing and cooling preserved in others? Similar studies performed on other monotonous intermediates may help in answering these important questions.

REFERENCES

Anderson, D.J. & Lindsley, D.H. (1988). Internally consistent solution models for Fe-Mg-Mn-Ti oxides: Fe-Ti oxides. *American Mineralogist* **73**, 714-726.

Anderson, D.J., Lindsley, D.H. & Davidson, P.M. (1993). QUILF: a PASCAL program to assess equilibrium among Fe-Mg-Ti oxides, pyroxenes, olivine, and quartz. *Computers and Geosciences* **19**, 1333-1350.

Anderson, J.L. & Smith, D.R. (1995). The effects of temperature and fO_2 on the Al-in Hornblende barometer. *American Mineralogist* **80**, 549-559.

Bachmann, O. & Bergantz, G. W. (2006). Gas percolation in upper-crustal silicic crystal mushes as a mechanism for upward heat advection and rejuvenation of near-solidus magma bodies. *Journal of Volcanology and Geothermal Research* **149,** 85–102.

Bachmann, O. & Bergantz, G. W. (2003). Rejuvenation of the Fish Canyon magma body: A window into the evolution of large-volume silicic magma systems. *Geology* **31**, 789-792.

Bachmann, O., Dungan, M.A. & Lipman, P.W. (2002). The Fish Canyon magma body, San Juan volcanic field, Colorado: rejuvenation and eruption of an upper crustal batholith. *Journal of Petrology* **43**, 1469-1503.

Bachmann, O. & Dungan, M.A. (2002). Temperature-induced Al-zoning in hornblendes of the Fish Canyon magma, Colorado. *American Mineralogist* **87**, 1062-1076.

Bacon, C.R. & Hirschmann, M.M. (1988). Mg/Mn partitioning as a test for equilibrium between coexisting Fe-Ti oxides. *American Mineralogist* **73**, 57-61.

Best, M.G. (2003). *Igneous and Metamorphic Petrology – 2nd edition.* Blackwell Science Ltd.: Blackwell Publishing, U.S.A.

Best, M.G. & Christiansen, E.H. (1991). Limited extension during peak Tertiary volcanism, Great Basin of Nevada and Utah. *Journal of Geophysical Research* **96**, 13509-13528.

Best, M.G., Christiansen, E.H. & Blank, H.R. Jr. (1989). Oligocene caldera complex and the calc-alkaline tuffs and lavas of the Indian Peak volcanic field, Nevada and Utah. *Geological Society of America Bulletin* **101**, 1076-1090.

Blundy, J.D. & Holland, T.J. (1990). Calcic amphibole equilibria and a new amphibole plagioclase geothermometer. *Contributions to Mineralogy and Petrology* **104**, 208-224.

Christiansen, E.H. (2005). Contrasting processes in silicic magma chambers: Evidence from very large volume ignimbrites. *Geological Magazine* **142**, 669-681.

Cosca, M.A., Essene, E.J. & Bowman, J.R. (1991). Complete chemical analyses of metamorphic hornblendes: implications for normalizations, calculated H_20 activities, and thermobarometry. *Contributions to Mineralogy and Petrology* **108,** 472-484.

de Silva, S.L., Self, S., Francis, P.W., Drake, R .E. & Ramirez, Carlos R. (1994). Effusive silicic volcanism in the Central Andes: The Chao dacite and other young lavas of the Altiplano-Puna Volcanic Complex. *Journal of Geophysical Research* **99**, 17,805–17,825.

de Silva, S.L. (1989). Geochronology and stratigraphy of ignimbrites from the 21 30' to 23 30'S portion of the central Andes of N. Chile. *Journal of Volcanology and Geothermal Research* **65**, 111-118.

Francis, P.W., Sparks, R.S.J., Hawkesworth, C.J., Thorpe, R.S., Pyle, D.M., Tait, S.R., Mantovani, M.S. & McDermott, F. (1989). Petrology and geochemistry of volcanic rocks of the Cerro Galan caldera, northwest Argentina. *Geological Magazine* **126**, 515-547.

Frost, B.R., Barnes, C.G., Collins, W.J., Arculus, R.J., Ellis, D.J. & Frost, C.D. (2001). A geochemical classification for granitic rocks. *Journal of Petrology* **42**, 2033-2048.

Ghiorso M.S. & Evans B.W. (in press). Thermodynamics of rhombohedral oxide solid solutions and a revision of the Fe-Ti two-oxide geothermometer and oxygen-barometer. *American Journal of Science*.

Ghiorso, M.S. & Sack, R.O. (1991). Fe-Ti oxide geothermometry: Thermodynamic formulation and the estimation of intensive variables in silicic magmas. *Contributions to Mineralogy and Petrology* **108**, 485-510.

Hart, G.L., Johnson, C.M., Hildreth, W. & Shirey, S.B. (2003). New osmium isotope evidence for intracrustal recycling of crustal domains with discrete ages. *Geology* **31**, 427-430.

Hammarstrom, J.M. & Zen, E. (1986). Aluminum in hornblende: An empirical igneous geobarometer. *American Mineralogist* **71**, 1297-1313

Henry, D.J., Guidotti, C.V. & Thomson, J.A. (2005). The Ti-saturation surface for low-to-medium pressure metapelitic biotites: Implications for geothermometry and Ti-substitution mechanisms. *American Mineralogist* **90**, 316-328.

Hildreth, W. (1981). Gradients in silicic magma chambers: Implications for lithospheric magmatism. *Journal of Geophysical Research* **86**, 10153-10192.

Holland, T. & Blundy, J. (1994). Non-ideal interactions in calcic amphiboles and their bearing on amphibole-plagioclase thermometry. *Contributions to Mineralogy and Petrology* **116**, 433-447

Hollister, L.S., Grissom, G.C., Peters, E.K., Stowell, H.H. & Sisson, V.B. (1987). Confirmation of the empirical correlation of Al in hornblende with pressure of solidification of calc-alkaline plutons. *American Mineralogist* **72**, 231-239.

Humphreys, E.D. (1995). Post-Laramide removal of the Farallon slab, western United States. *Geology* **23**, 987-990.

Humphreys, M.C., Blundy, J.D. & Sparks, R.S. (2006). Magma evolution and open system processes at Shiveluch Volcano: Insights from phenocryst zoning. *Journal of Petrology* **47**, 2303-2334.

Johnson, M.C. & Rutherford, M.J. (1989a). Experimentally determined conditions in the Fish Canyon Tuff, Colorado, magma chamber. *Journal of Petrology* **30**, 711-737.

Johnson, M.C. & Rutherford, M.J. (1989b). Experimental calibration of the aluminum in hornblende geobarometer with application to Long Valley Caldera (California). *Geology* **17**, 837-841.

Kennedy, B. & Stix, J. (2007). Magmatic processes associated with caldera collapse at Ossipee ring dyke, New Hampshire. *Geological Society of America Bulletin* **119**, 3–17.

Leake, B.E., Woolley, A.R., Arps, C.E.S., Birch, W.D., Gilbert, M.C., Grice, J.D., Hawthorne, F.C., Kato, A., Kisch, H.J., Krivovichev, V.G., Linthout, K., Laird, J., Mandarino, J.A., Maresch, W.V., Nickel, E.H., Rock, N.M.S., Schumacher, J.C., Smith, D.C., Stephenson, N.C.N., Ungaretti, L., Whittaker, E.J.W. & Youzhi, G. (1997). Nomenclature of amphiboles: Report of the subcommittee on amphiboles of the International Mineralogical Association, commission on new minerals and mineral names. *The Canadian Mineralogist* **35**, 219-246.

Le Bas, M.J., Le Maitre, R.W., Streckeisen, A. & Zanettin, B. (1986). A Chemical Classification of Volcanic Rocks Based on the Total Alkali-Silica Diagram. *Journal of Petrology* **27**, 745-750.

Lindsay, J.M., Schmitt, A.K., Trumbull, R B., de Silva, S.L., Siebel, W. & Emmermann, R. (2001). Magmatic evolution of the La Pacana Caldera system, Central Andes, Chile: Compositional variation of two cogenetic, large-volume felsic ignimbrites. *Journal of Petrology* **42**, 459–486.

Lipman, P.W. (2007). Incremental assembly and prolonged consolidation of the Cordilleran magma chambers: Evidence from the Southern Rocky Mountain volcanic field. *Geosphere* **3**, 42-70.

Luhr, J.F., Carmichael, I.S.E. & Varekamp, J.C. (1985). The 1982 eruptions of El Chichon Volcano, Chiapas, Mexico: Mineralogy and petrology of the anhydrite bearing pumice. *Journal of Volcanology and Geothermal Research* **23**, 69-108.

Maughan, L., Christiansen, E.H., Best, M.G. & Gromme, S. (2002). The Oligocene Lund Tuff, Great Basin, USA: A very large volume monotonous intermediate. *Journal of Volcanology and Geothermal Research* **113**, 129-157.

McDonough, W.F. & Sun, S.S. (1995). The composition of the Earth. *Chemical Geology* **120**, 223–253.

Molloy, C., Shane, P. & Nairn, I. (2008). Pre-eruption thermal rejuvenation and stirring of a partly crystalline rhyolite pluton revealed by the Earthquake Flat Pyroclastics deposits, New Zealand. *Journal of the Geological Society* **65,** 435-448.

Morimoto, N., Fabries, J., Ferguson, A.K., Ginzburg, I.V., Ross, M., Seifert, F. A., Zussman, J., Aoki, K. & Gottardi, G. (1988). Nomenclature of pyroxenes. *American Mineralogist* **73**, 1123-1133.

Nusbaum, R, L. (1990). Evidence for magma hybridization for the voluminous 29.5 Ma Wah Wah Springs Formation, Utah and Nevada, U.S.A. *Journal of Volcanology and Geothermal Research* **40**, 245-256.

Parat, F., Dungan, M.A. & Lipman, P.W. (2008). Contemporaneous Trachyandesitic and Calc-alkaline Volcanism of the Huerto Andesite, San Juan Volcanic Field, Colorado, USA. *Journal of Petrology* **46**, 859–891.

Pearce, J.A., Harris, N.B. & Tindle, A.G. (1984). Trace element discrimination diagrams for the tectonic interpretation of granitic rocks. *Journal of Petrology* **25**, 956–983.

Putirka, K.D., Mikaelian, H., Ryerson, F. & Shaw, H. (2003). New clinopyroxene-liquid thermobarometers for mafic, evolved, and volatile-bearing lava compositions, with applications to lavas from Tibet and the Snake River Plain, Idaho. *American Mineralogist* **88**, 1542–1554.

Putirka, K.D. (2005). Igneous thermometers and barometers based on plagioclase + liquid equilibria: Tests of some existing models and new calibrations. *American Mineralogist* **90**, 336-346.

Righter, K. & Carmichael, I.S.E. (1996). Phase equilibria of phlogopite lamprophyres from western Mexico; biotite-liquid equilibria and P-T estimates for biotite-bearing igneous rocks. *Contributions to Mineralogy and Petrology* **123**, 1-21.

Sauerzapf, U., Lattard, D., Burchard, M. & Engelmann, R. (2008). The Titanomagnetite Ilmenite Equilibrium: New Experimental Data and Thermooxybarometric Application to the Crystallization of Basic to Intermediate Rocks. *Journal of Petrology* **00**, 1-25.

Schmidt, M.W. (1992). Amphibole composition in a tonalite as a function of pressure: An experimental calibration of the Al-in-hornblende barometer. *Contributions to Mineralogy and Petrology* **110**, 304-310.

Spear, F.S. (1981). An experimental study of the hornblende stability and compositional variability in amphibolite. *American Journal of Science* **281,** 697-734.

Stormer, J.C. (1983). The effects of recalculation on estimates of temperature and oxygen fugacity from analyses of multicomponent iron-titanium oxides. *American Mineralogist* **68**, 586-594.

Swanson, S.E. & Fenn, P.M. (1986). Quartz crystallization in igneous rocks. *American Mineralogist* **71**, 331-342.

Wark, D., Hildreth, W., Spear, F., Cherniak, D. & Watson, E. (2007). Pre-eruption recharge of the Bishop magma system. *Geology* **35**, 235-238.

Whitney, J.A. & Stormer, J.C. (1985). Mineralogy, petrology, and magmatic conditions from the Fish Canyon Tuff, central San Juan volcanic field, Colorado. *Journal of Petrology* **26**, 726–762.

APPENDIX A

Sample descriptions for the FRSC-8-0, GOUGE-1V, HAM-6V, MIN-3V, PANGNW-1A, and PIERSON-3-78-5 samples.

FRSC-8-0

38° 28’ 44” N, 113° 29’ 51” W

Dark gray, porphyritic, vitrophyric welded, dacitic, tuff. 48% eutaxitic, glass matrix. Phenocrysts consist of 20% subhedral plagioclase (0.25-4mm) displaying oscillatory zoning and simple and polysynthetic twinning, 15% subhedral to euhedral hornblende (0.25-2mm) often displaying simple twinning, 7% subhedral, fractured, embayed quartz (0.5-1.75mm), 5% euhedral, tabular biotite (0.25-1.75mm), 3% euhedral Fe-Ti oxides (up to 0.5mm), and about 1 % each of anhedral to subhedral clinopyroxene and orthopyroxene (0.25-0.75mm). Plagioclase and biotite show flow alignment.

GOUGE-1V

38° 34’ 53” N, 114° 25’ 43” W

Dark gray to black, porphyritic, vitrophyric, welded, dacitic, tuff. 66% eutaxitic, glass matrix. Phenocrysts consist of 15% subhedral plagioclase (0.25-1.25mm) displaying oscillatory zoning and simple and polysynthetic twinning, 7% subhedral to euhedral hornblende (0.25-1.25mm) often displaying simple twinning, 6% euhedral, tabular biotite (0.5-1.5mm), 3% subhedral to euhedral Fe-Ti oxides (up to 0.5mm), 2% anhedral, fractured quartz (0.5-0.75mm), and less than 1 % each of anhedral clinopyroxene and orthopyroxene (0.25-0.5mm). Plagioclase and biotite show flow alignment.

HAM-6V

38° 29’ 33” N, 114° 3’ 13” W

Dark gray to black, porphyritic, vitrophyric, welded, dacitic, tuff. 54% eutaxitic, glass matrix. Phenocrysts consist of 20% subhedral plagioclase (0.25-1.75mm) displaying oscillatory zoning and simple and polysynthetic twinning, 15% subhedral to euhedral

hornblende (0.25-2.5mm) often displaying simple twinning, 7% euhedral, tabular biotite (0.25-2.25mm), 3% subhedral Fe-Ti oxides (up to 0.5mm), and less than 1 % each of anhedral clinopyroxene and orthopyroxene (0.25-0.5mm). No quartz is found. Plagioclase and biotite show flow alignment.

MIN-3V

38° 16’ 18” N, 113° 52’ 55” W

Gray, porphyritic, welded, dacitic, tuff. 43% slightly altered vitrophyric matrix containing 2% pumice lapilli (2-5mm) and rare lithic fragments (2mm). Phenocrysts consist of 20% subhedral to euhedral plagioclase (0.25-2.0mm) displaying oscillatory zoning, simple and polysynthetic twinning and secondary alteration to clay, 15% subhedral to euhedral hornblende (0.25-1.5mm) often displaying simple twinning and in some cases oscillatory zoning is seen optically, 10% subhedral to euhedral, quartz (0.25-1.75mm), 5% subhedral, tabular biotite (0.25-1.5mm) which is highly altered, 5% subhedral to euhedral Fe-Ti oxides (0.25-1.0mm), and about 1 % anhedral clinopyroxene (0.25-0.5mm) displaying some simple twinning. No orthopyroxene was found.

PANGNW-1A

37° 58’ 18” N, 112° 26’ 7” W

Gray, porphyritic, welded, dacitic, tuff. 52% eutaxitic, ashy matrix containing 3% fiamme (5-20mm) and rare lithic fragments (2mm). Phenocrysts consist of 20% subhedral to euhedral plagioclase (0.25-2.0mm) displaying oscillatory zoning and simple and polysynthetic twinning, 10% subhedral to euhedral hornblende (0.25-1.5mm) often displaying simple twinning, 7% subhedral, tabular biotite (0.25-2.5mm), 5% subhedral, quartz (0.25-1.25mm), 3% subhedral to euhedral Fe-Ti oxides (0.25-0.75mm), 2% of

subhedral clinopyroxene (0.25-1.5mm). Plagioclase and biotite show flow alignment. No innate orthopyroxene was found. Rare holocrystalline, xenocyrstic clots of plagioclase, hornblende, clinopyroxene, and orthopyroxene were found.

PIERSON-3-78-5

38° 3’ 0” N, 114° 15’ 30” W

Gray, porphyritic, vitrophyric welded, dacitic, tuff. 47% eutaxitic, ashy matrix containing 1% lithic fragments (2mm). Phenocrysts consist of 25% subhedral to euhedral plagioclase (0.25-2.25mm) displaying oscillatory zoning and simple and polysynthetic twinning, 20% subhedral to euhedral hornblende (0.25-2.25mm) often displaying simple twinning, 5% subhedral, tabular biotite (0.25-2.5mm) which is altered, 3% subhedral Fe-Ti oxides (0.25-1.0mm), <1% anhedral clinopyroxene (0.25mm). No quartz is found. Plagioclase and biotite show flow alignment.

APPENDIX B

Complete chemical analyses from each major phase can be accessed electronically as an Excel document attached to the .pdf form of this document. To view attachments choose View > Navigation Panel > Attachments

APPENDIX C

Chemical profiles across each plagioclase grain in which traverses were made.

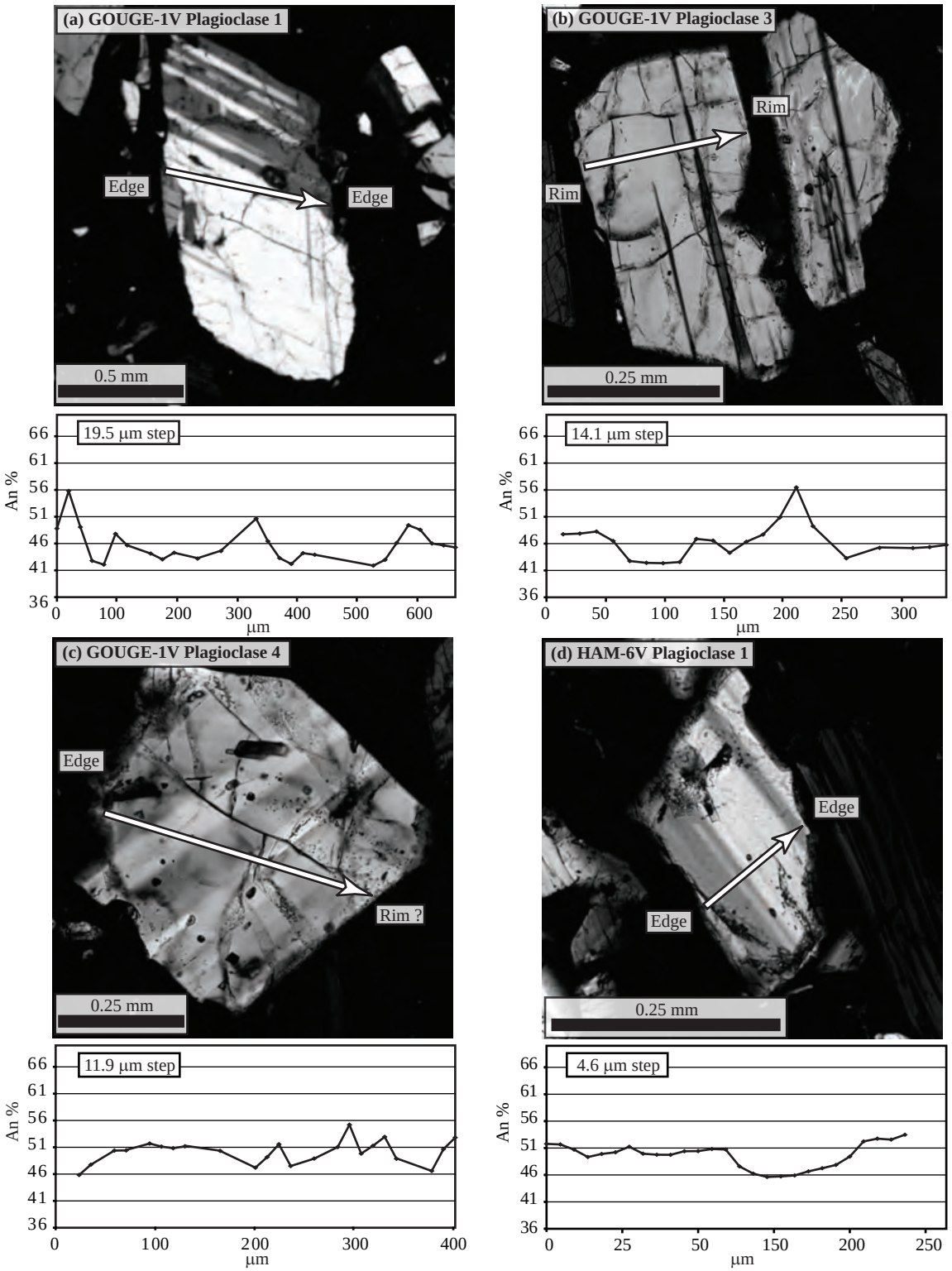

Fig 1. Plagioclase composition profiles show oscillations and an overall decrease in An content from cores to rims.

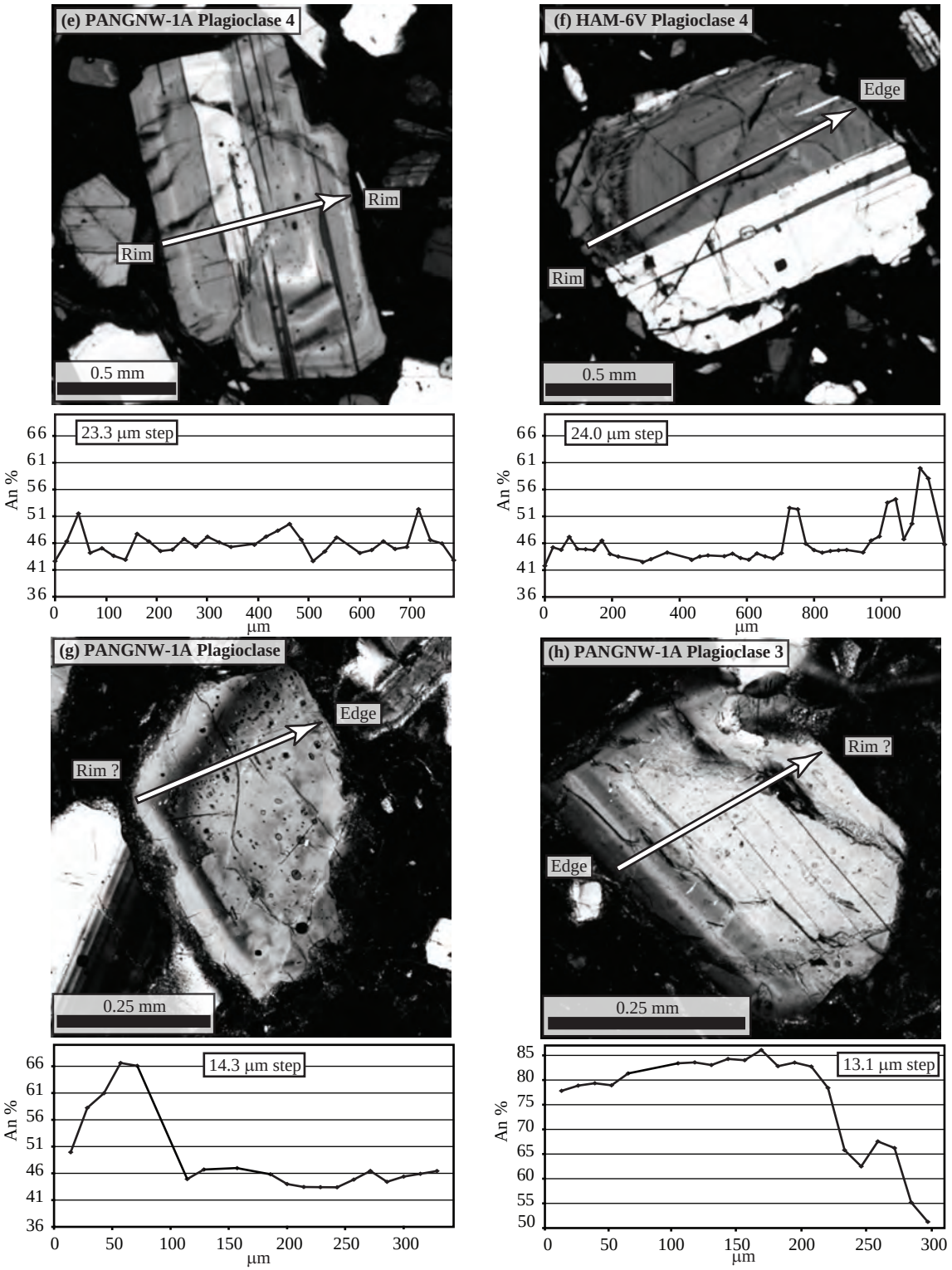

Fig 2. Plagioclase composition profiles show oscillations and an overall decrease in An content from cores to rims.

APPENDIX D

Chemical profiles across each hornblende grain in which traverses were made.

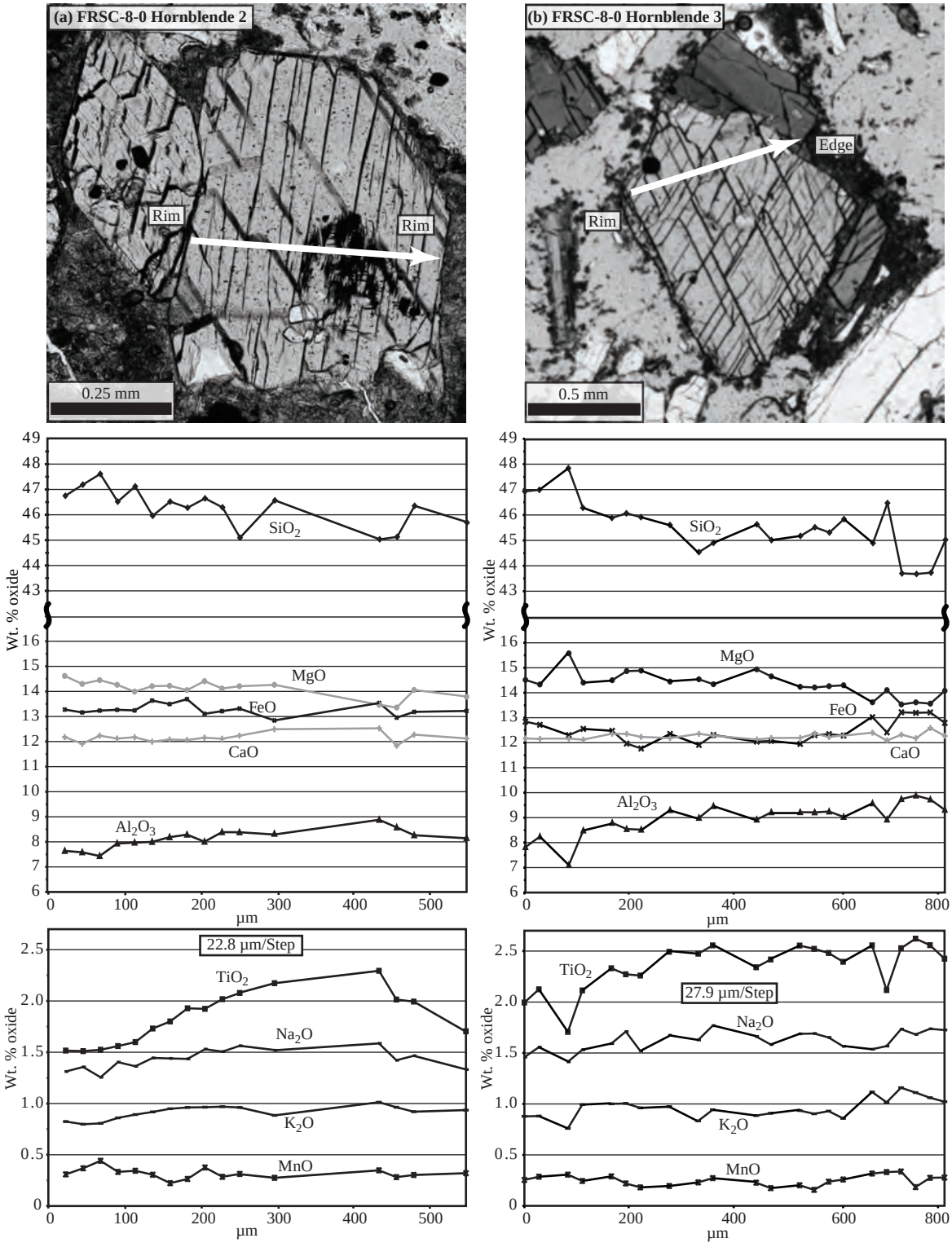

Fig. 1. Hornblende traverses across two euhedral grains. These traverses show a decrease in Al_2O_3 and TiO_2 from core to rim indicating normal zonation and a cooling and crystallizing magma. (a) and (b) hornblendes from the FRSC-8-0 locality.

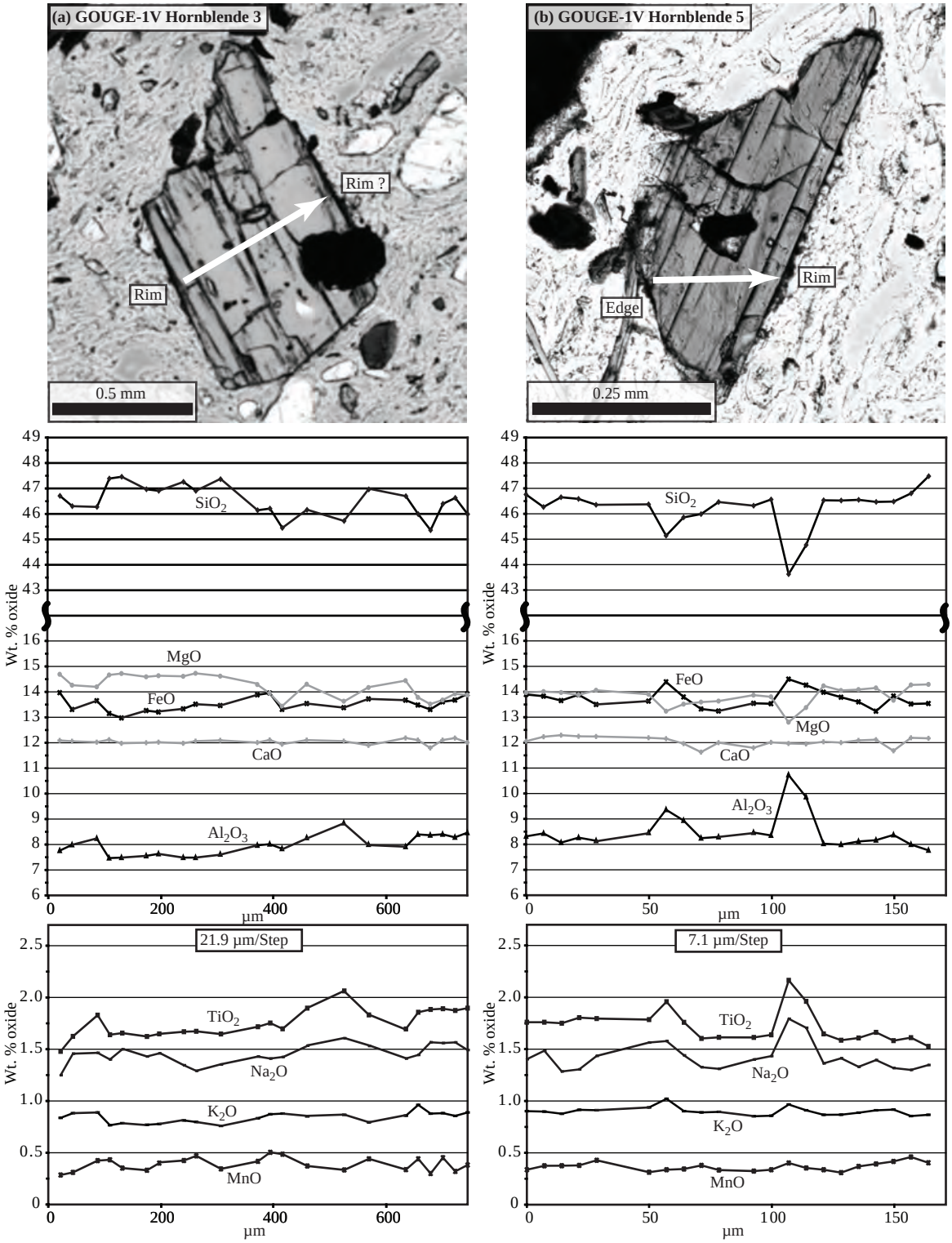

Fig. 2. Hornblende traverses across two euhedral grains. These traverses show a decrease in Al_2O_3 and TiO_2 from core to rim indicating normal zonation and a cooling and crystallizing magma. (a) and (b) hornblendes from the GOUGE-1V locality.

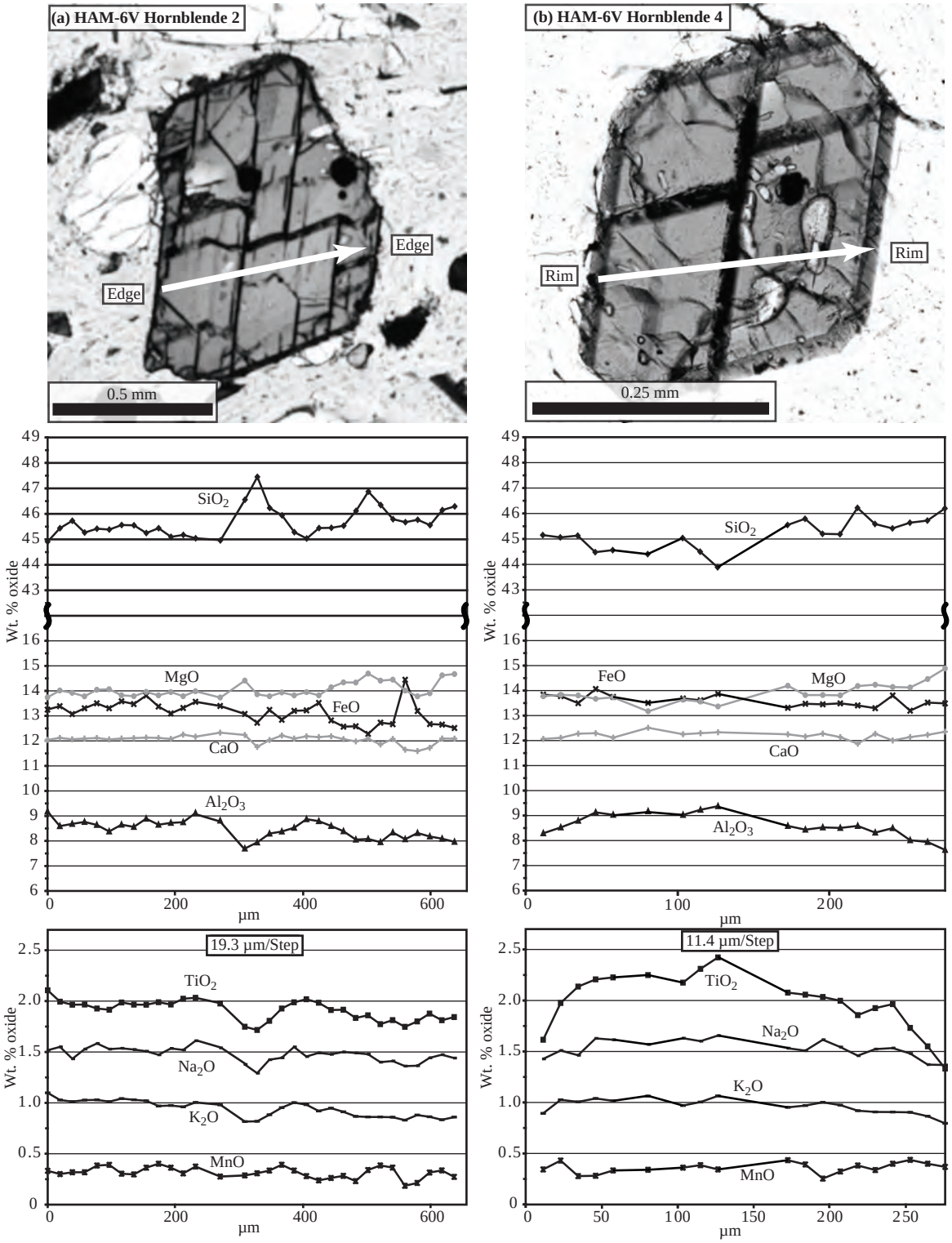

Fig. 3. Hornblende traverses across two grains. These traverses show a decrease in Al_2O_3 and TiO_2 from core to rim/edge indicating normal zonation and a cooling and crystallizing magma. (a) and (b) hornblendes from the HAM-6V locality.

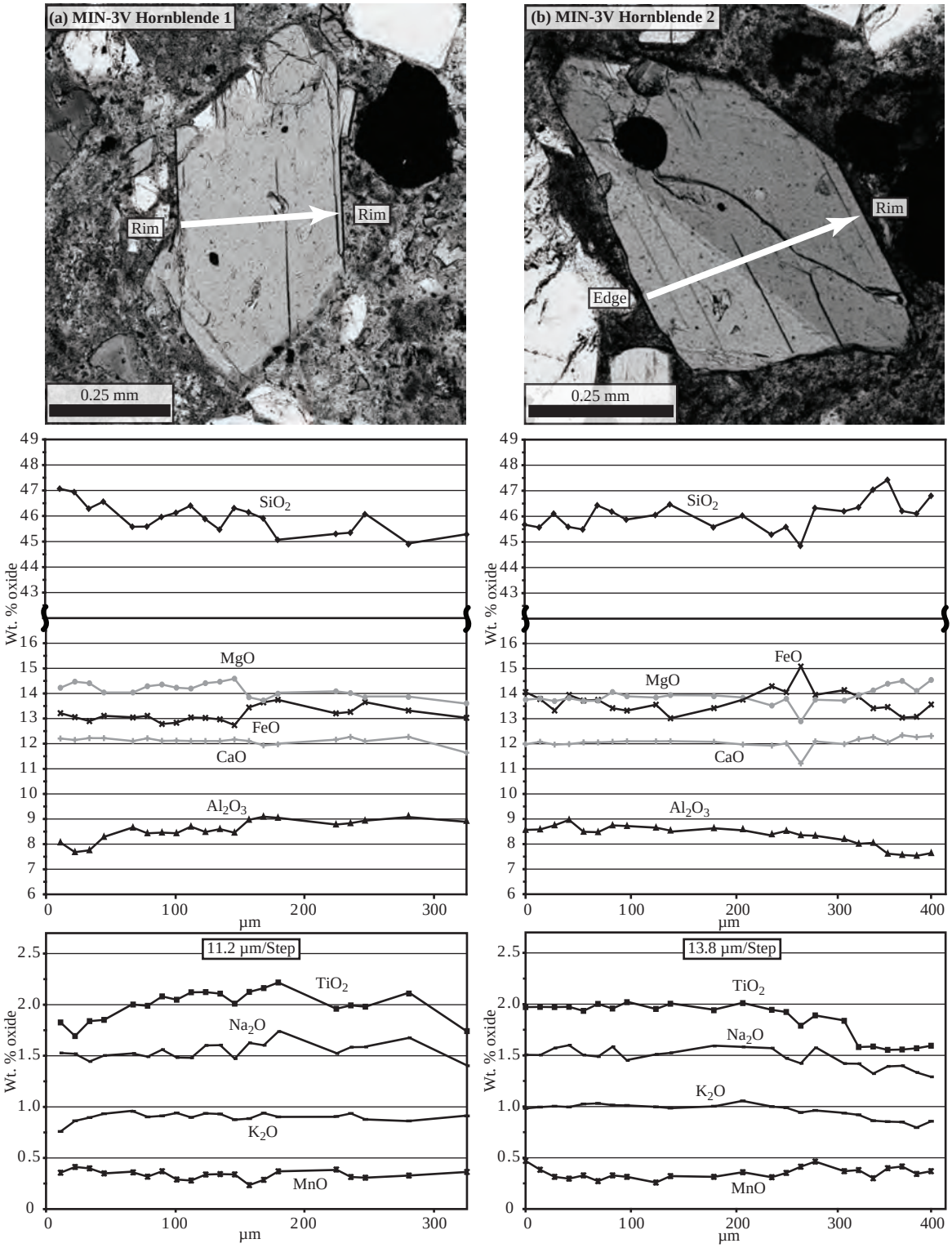

Fig. 4. Hornblende traverses across two euhedral grains. These traverses show a decrease in Al_2O_3 and TiO_2 from core to rim indicating normal zonation and a cooling and crystallizing magma. (a) and (b) hornblendes from the MIN-3V locality.

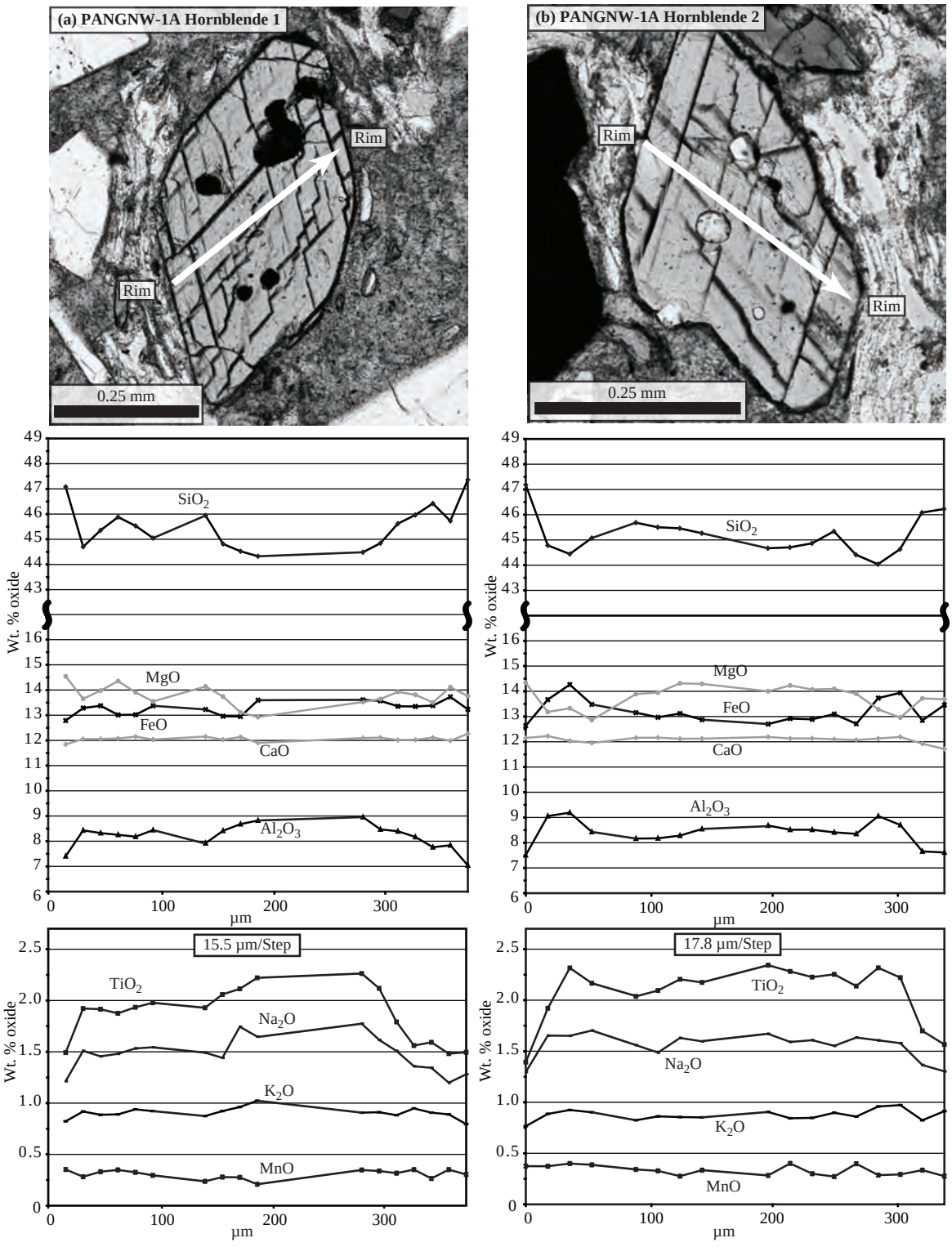

Fig. 5. Hornblende traverses across two euhedral grains. These traverses show a decrease in Al_2O_3 and TiO_2 from core to rim indicating normal zonation and a cooling and crystallizing magma. (a) and (b) hornblendes from the PANGNW-1A locality.

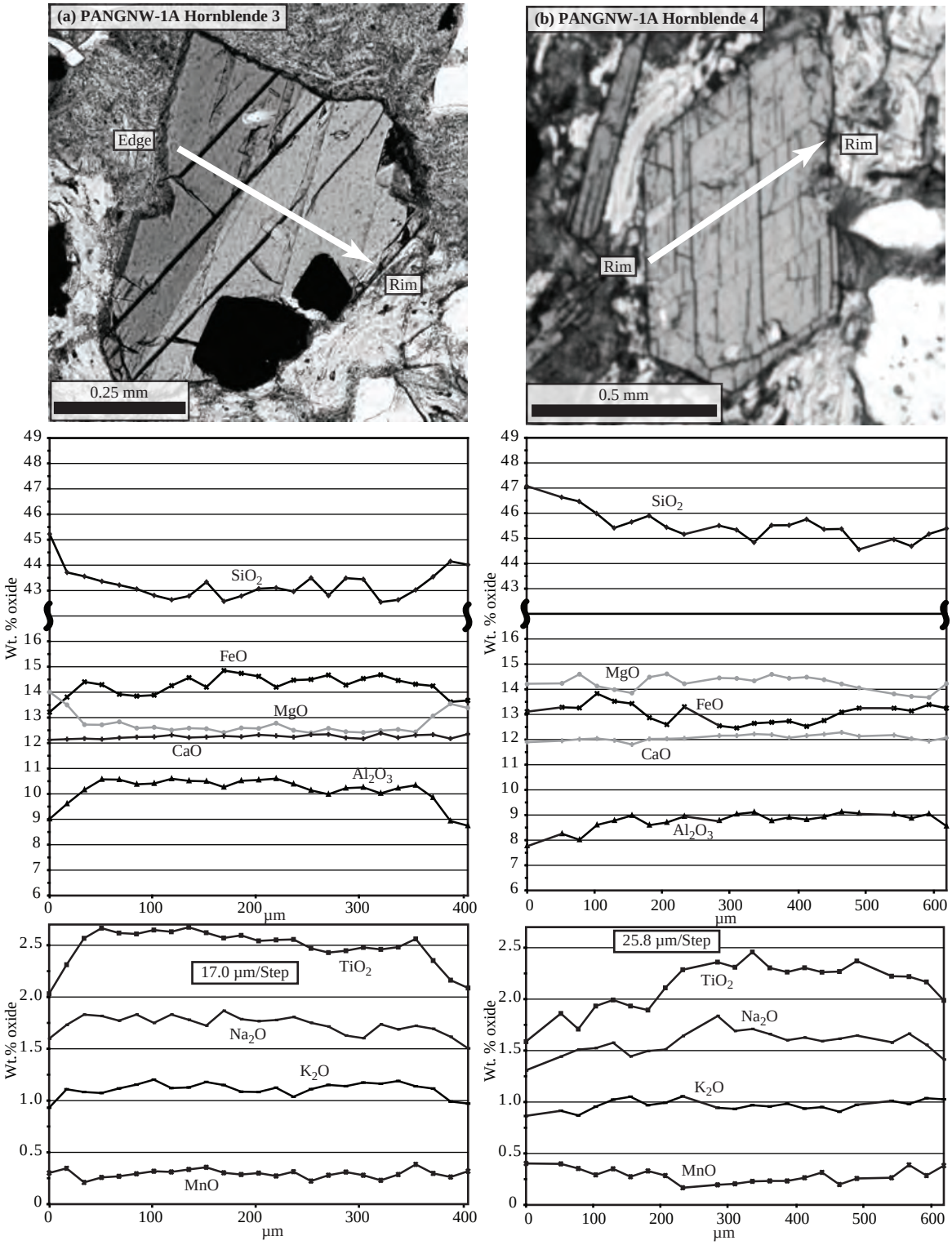

Fig. 6. Hornblende traverses across two euhedral grains. These traverses show a decrease in Al_2O_3 and TiO_2 from core to rim indicating normal zonation and a cooling and crystallizing magma. (a) and (b) hornblendes from the PANGNW-1A locality.

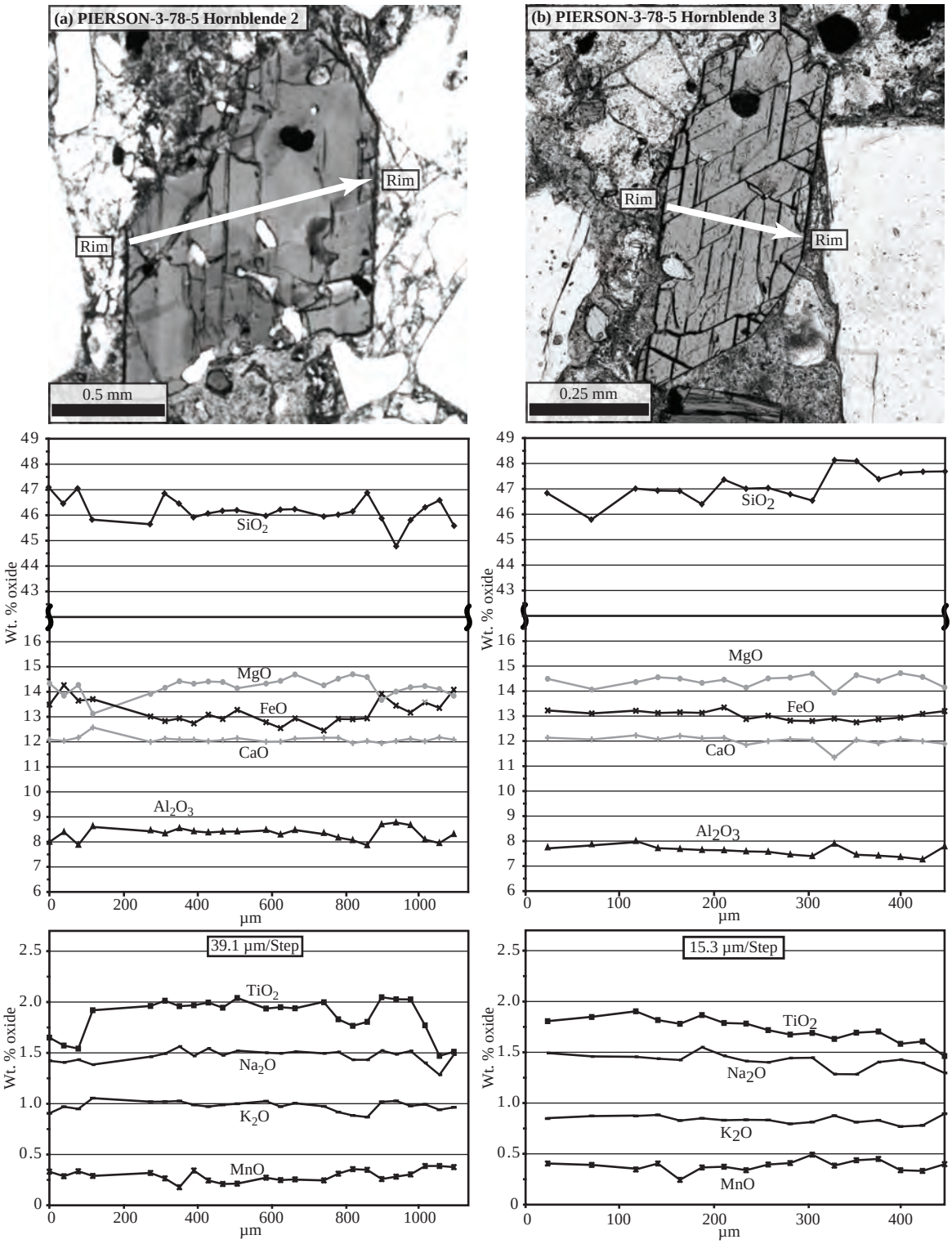

Fig. 7. Hornblende traverses across two euhedral grains. These traverses show a decrease in Al_2O_3 and TiO_2 from core to rim indicating normal zonation and a cooling and crystallizing magma. (a) and (b) hornblende grains from the PIERSON-3-78-5 locality.

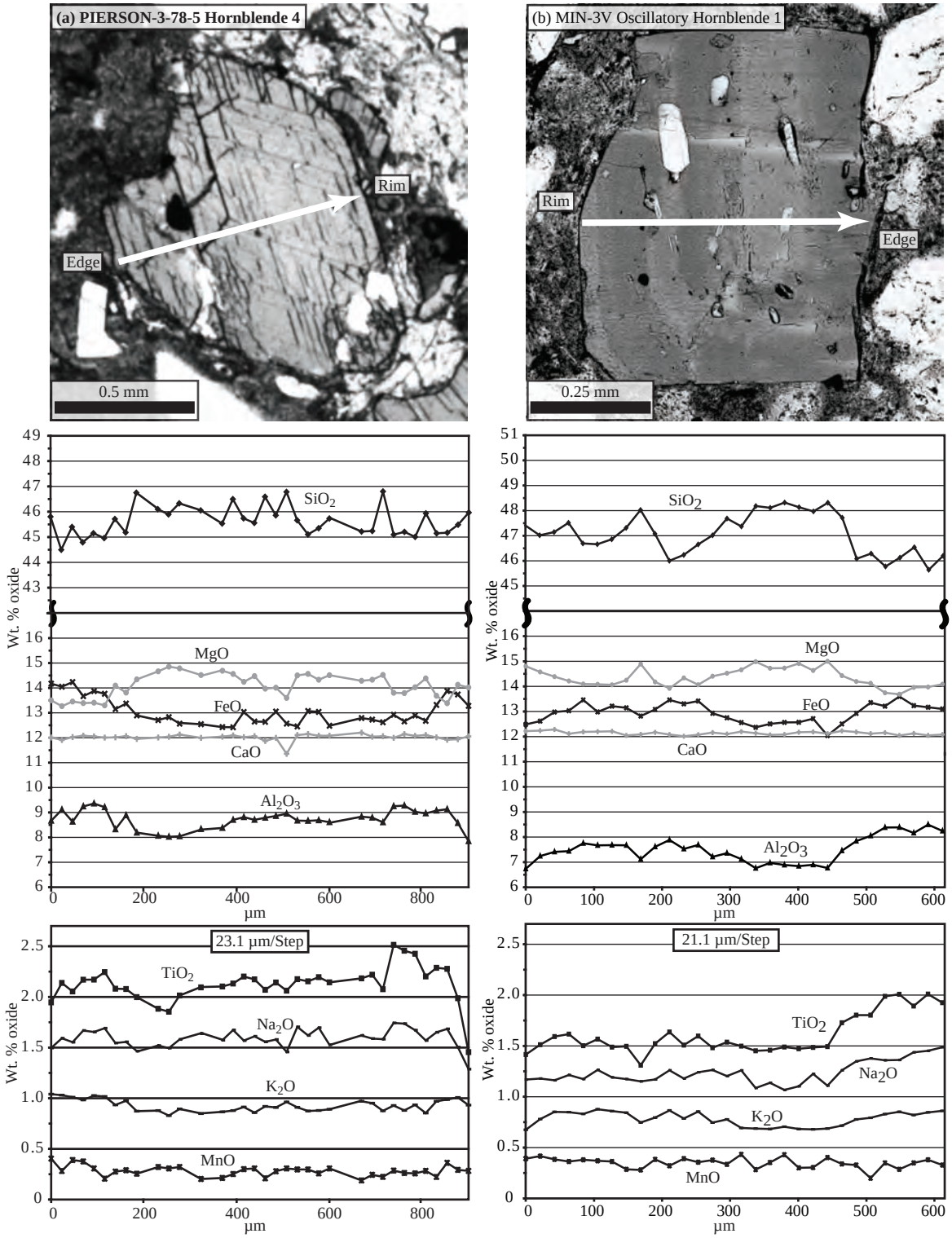

Fig. 8. Hornblende traverses across two subhedral grains. Both traverses show a decrease in Al_2O_3 and TiO_2 from core to rim indicating normal zonation and a cooling and crystallizing magma. (a) A hornblende from the PIERSON-3-78-5 locality. (b) An oscillatory hornblende grain from the MIN-3V locality.

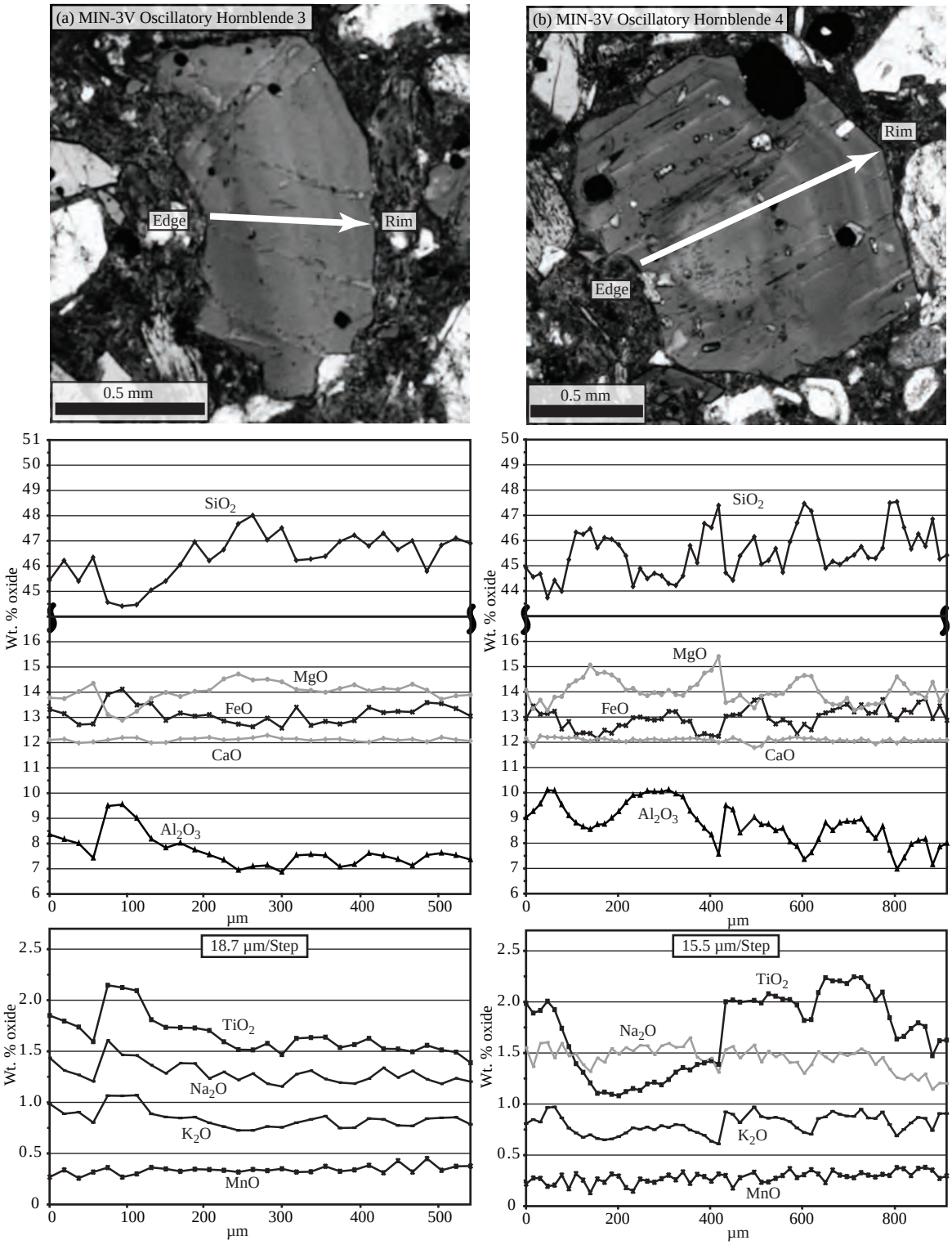

Fig. 9. Hornblende traverses across two oscillatory grains. These traverses show a decrease in Al_2O_3 and TiO_2 from core to rim indicating normal zonation and a cooling and crystallizing magma. (a) and (b) hornblende grains from the MIN-3V locality.

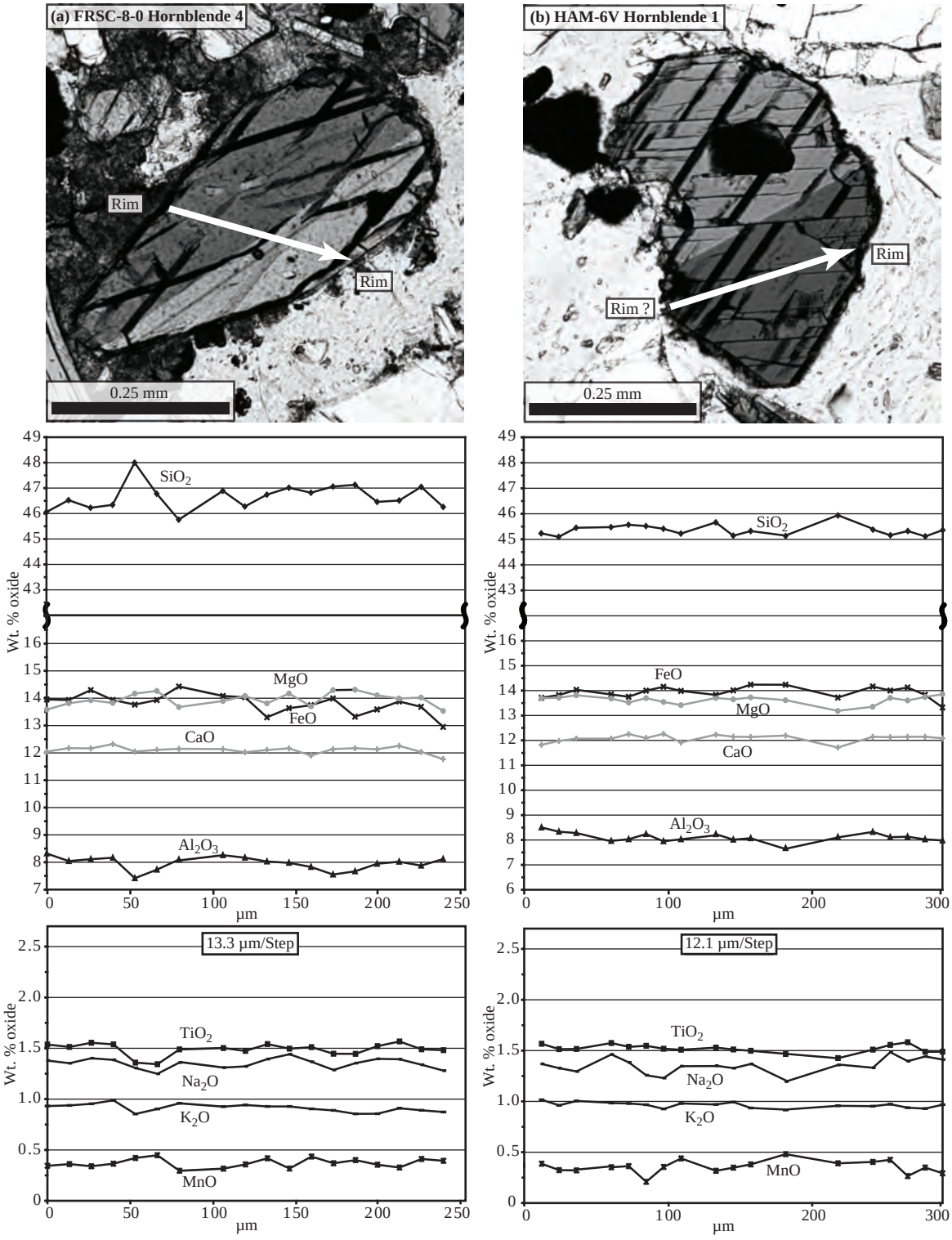

Fig. 10. Hornblende traverses across two euhedral grains. These traverses show a flat pattern with little zonation. (a) A hornblende from the FRSC-8-0 locality. (b) A hornblende grain from the HAM-6V locality.

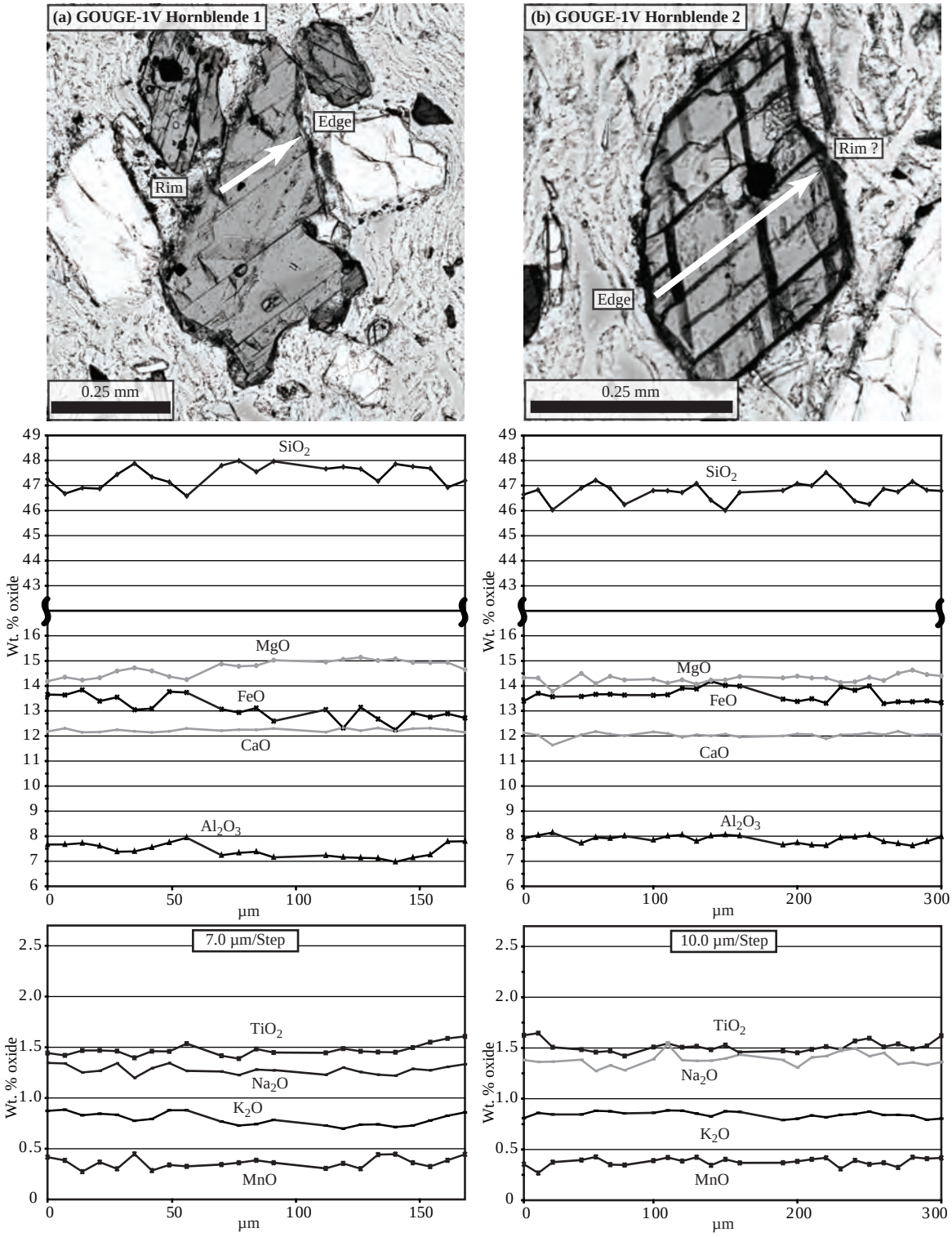

Fig. 11. Hornblende traverses across two subhedral grains. These traverses show little zonation across the grain. (a) and (b) hornblende grains from the GOUGE-1V locality.